The following manuscript was unavailable at the time of publication.

ASSESSMENT OF TOXIC EMISSIONS FROM THE CARDINAL STATION

G. England
Energy Research & Environmental Research Corporation
18 Mason Street
Irvine, CA 92718

Please contact author(s) for a copy of this paper.

AN INNOVATIVE CONTINUOUS EMISSIONS MONITOR FOR AIR TOXIC METALS

DR. ANDREW D. SAPPEY

PRINCIPAL INVESTIGATOR

ADA TECHNOLOGIES

DR. DAVID HYATT

SENIOR RESEARCH CHEMIST

CHEMICAL AND METAL INDUSTRIES

MR. FRANK SAGAN

SENIOR TECHNICIAN

ADA TECHNOLOGIES

Background and Technical Approach

The Clean Air Act amendments of 1990 defined 189 individual hazardous air pollutants which must be monitored and controlled. Of the 189 listed species, 11 are metals including arsenic, beryllium, mercury, antimony, cadmium, chromium, cobalt, lead, manganese, nickel, and selenium. The current method of monitoring these species as components of flue gas requires sampling of the waste stream followed by analysis for the target metals with separate analytical procedures. The assay typically requires sample preparation and then analysis by a well-equipped analytical laboratory using, perhaps, several techniques. This facility may be distant from the waste stream and have a significant backlog. The results of the analysis may take several weeks to months to obtain, and significant environmental insult can occur in the interim. Consequently, there is a real need for a continuous, real-time monitor for these metal air toxic species. There is no such technology presently in existence.

ADA Technologies is currently developing an metal air toxics CEM for a DOE Phase I SBIR program. Detection of all 11 metal air toxics simultaneously is complicated by the fact that some of the species such as chromium, nickel, and beryllium are present in the effluent as components of the fly ash, while others such as mercury may be adsorbed on the fly ash or present in the gas phase as an aerosol. In addition, the metals may be speciated as chlorides, oxides, nitrates, etc. Consequently, the CEM must be sensitive to the metal species regardless of physical or chemical matrix effects.

The ADA approach to CEM development relies on inductively coupled plasma (ICP) - emission spectroscopy. We have combined this very sensitive analytical technique with photodiode array (PDA) technology which allows us to detect many metal species simultaneously. The high temperature of the ICP torch (typically 5000 - 10000 K for operation

with argon) vaporizes and dissociates the metal species and excites the resulting metal atoms and ions *electronically*. These electronic excitations produce line emission at characteristic wavelengths for each metal. Consequently, barring coincidental overlap of wavelengths for different metals, the plasma emission can be dispersed in a spectrograph and detected using a photodiode array multichannel detector. The PDA allows the user to monitor a *range* of wavelengths *simultaneously*. Thus, the ICP emission technique offers the promise of detecting multiple metal species, simultaneously and with excellent sensitivity.

In practice, the situation is complicated by several difficulties. In the field, the ICP-based CEM will need to operate with at least some, and preferably all, air since the flue gas to be sampled is, more or less, air. Operation with 100% air presents significant technological barriers. First, nominally, ICPs are designed to run with 100% argon. Meyer and Thompson at Battelle,[1] Seltzer and Green at China Lake,[2] and a cooperative French effort consisting of Nore, Gomes, Bacri, and Cabe[3] have all been successful at operating the ICP torch on a stream of 100% air. This requires a significant power input of about 2.1 kw at 40 - 64 MHz. In addition, the power supply must be modified to insure optimum coupling by adding capacitance to the coupling feedback loop.[1,2,3]

Achieving operation on 100% air, however, is the least of the difficulties. Introduction of air into the ICP creates a background emission signal consisting of mainly NO and OH emissions in the UV. The NO species are created from the oxygen and nitrogen in the air stream and excited by the electrons in the plasma. To produce OH radical, the air must be humid which, of course, will be the case with flue gas. The problem is that these species emit relatively broadband radiation over a significant wavelength range in which many of the target metals also emit. Thus, the noise level is increased for air operation and the amount of wavelength space free from interferences in the UV is significantly decreased.

Finally, operation with even small amounts of air cools the plasma temperature dramatically. The temperature is reduced from the normal 7,000 - 10,000 K operating range associated with argon to perhaps 3000 - 4500 K, not much higher than flame temperatures. This decrease is caused by dissociation of the air constituents, oxygen in particular, and subsequent radical reactions. Although the decrease in temperature is only a factor of approximately two, this effects the populations of the excited, emitting states exponentially through the Boltzmann factor. Thus, for the high lying excited states used for detection of arsenic and selenium which occur at 50,000 cm^{-1} (6.2 eV), a factor of two decrease in temperature translates into a factor of 3000 decrease in the population of the excited state. This translates into a correspondingly large decrease in signal (detection efficiency). For longer detection wavelengths the effect is not as severe, but still substantial. For example, at the lead detection wavelength (405 nm) the same factor of two decrease in temperature decreases the signal by a factor of 55. In addition, quantitative vaporization and dissociation of the metal species is not assured in the cooler parts of the air ICP torch which can cause significant errors.

Experimental Section and Results

The experimental apparatus used in this work is pictured in Figure 1. It consists of an RFPP Inc. 1.6 kW, 40.68 MHz rf power supply and ICP torch. The system was designed to run on argon. Emission from the torch was focused into an Oriel Multispec f/3.7, 1/8 meter spectrograph equipped with a 1200 lines/mm holographic grating with either a 1 inch diameter, 4 inch focal length quartz lens or an off - axis parabolic mirror, 2 inches in diameter with a 6 inch

focal length. A Hamamatsu S3904-1024Q linear diode array served as the detector. The detector has 1024 active diodes in a 1 inch array, and with the dispersion of the multispec, a 164 nm wavelength range can be acquired at any wavelength setting. In previous work, Seltzer and Green and Nore et al. used photomultiplier tubes as detectors which have the advantage of extraordinary sensitivity, but lack multichannel capability. Consequently, scanning monochromators must be used to obtain data which slows the acquisition process. Spectra are acquired and stored on a 386 PC. The PDA integrates the light impinging on each element for 3 secs before readout occurs; this constitutes a single spectrum. Additional averaging occurs on board the computer as explained below.

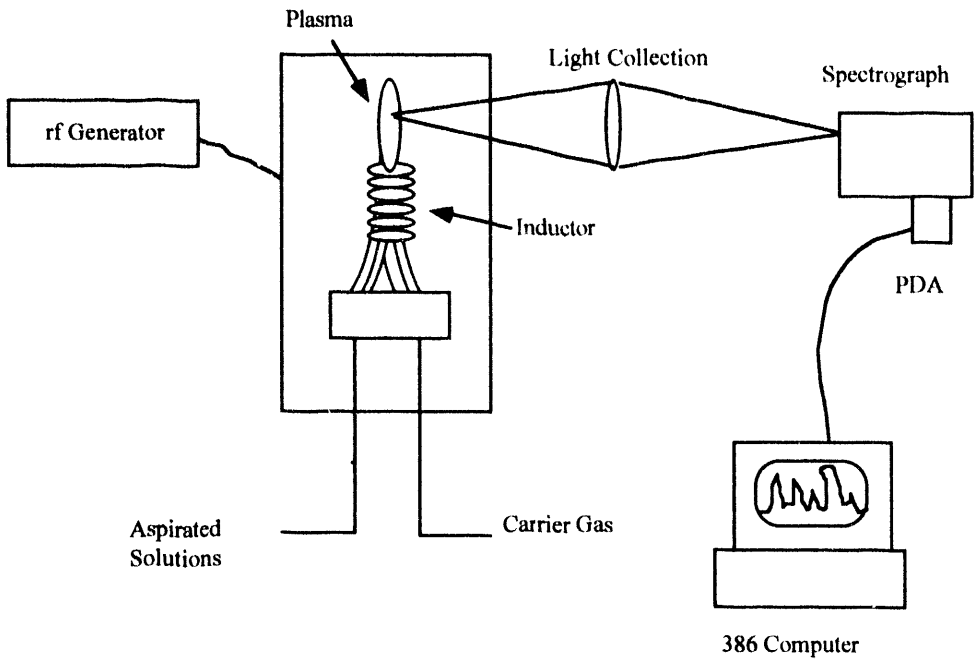

Figure 1: ICP Metals Apparatus

Due to the difficulty of producing known concentrations of metal samples in aerosol form or as components of fly ash, we determined sensitivity limits for eight of the target metals by aspirating standard solutions of known concentration into a nebulizer. This provides a source of metal at known concentration in the torch. By changing the concentration of the aspirated solution, we were able to determine sensitivity limits for each metal. In addition to the three second PDA integration time described above, a running average of 10 individual spectra is performed on board the computer to produce a single data point on the signal vs. time curve. At various times, solutions of known metal concentration are aspirated into the nebulizer and eventually introduced into the ICP. An experimental data set for chromium is shown in Figure 2. As a new spectrum is taken into the average, the spectrum which has already been included in ten averages is dropped. This slows the time response of the system to about 20 - 30 secs; however, the increase in signal to noise is dramatic.

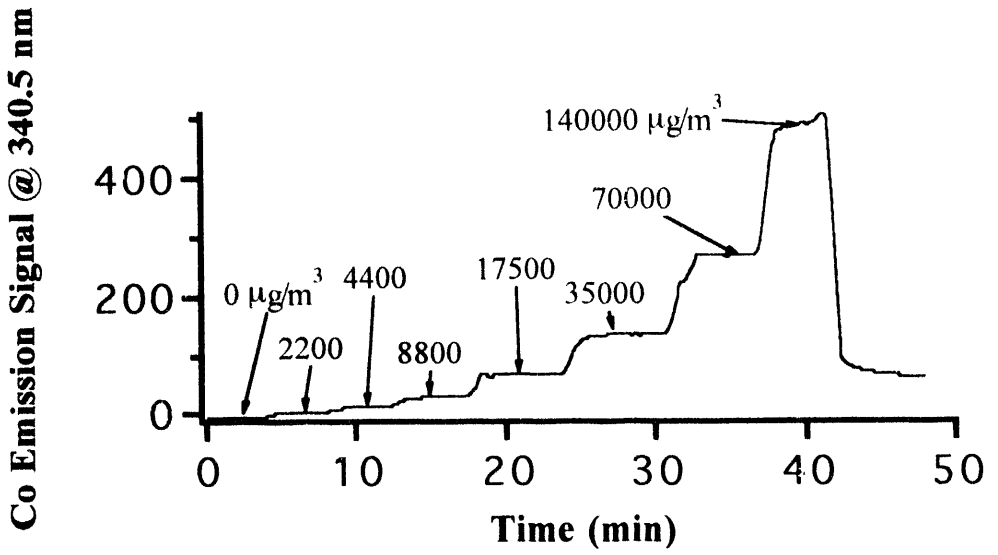

Figure 2: PDA signal counts vs. chromium concentration.

The average number of photodiode counts/sec is determined from the zero slope regions of Figure 2 for a given concentration and plotted vs. concentration as shown in Figure 3 for cobalt. Solutions are carefully prepared by the successive dilution method from standard 1000 μg/ml stock solutions (Johnson-Mathey) for each metal. We determined the ICP uptake rate to be 0.07 ml of stock solution/min. by measuring the mass loss of solution as a function of time at a carrier gas flow rate of 0.5 l/min. All calibration work was done at this flow rate. The detection sensitivity is then the slope of the emission response vs. concentration curve in Figure 3.

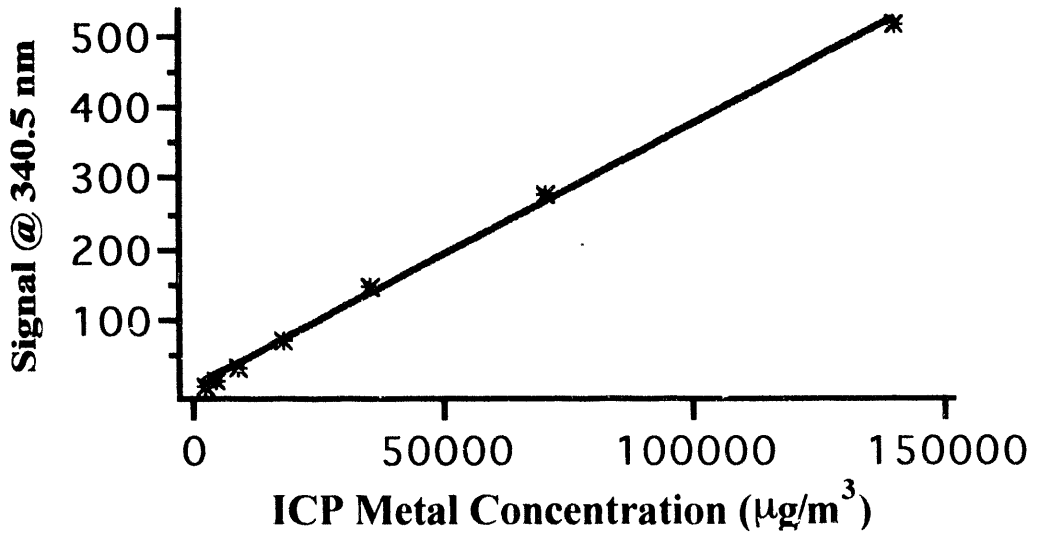

Figure 3: Calibration curve for Cobalt. Emission Signal vs. [Co] in the torch.

The concentration on the x - axis of Figure 3 is the concentration of the metal analyte *in the torch plume*. This number can easily be calculated from the ICP intake rate, the concentration of the aspirated solution, and the carrier gas flow rate. The concentration of the metal in the torch plume is used since the CEM must measure the concentration of a *gas phase* sample. The

detection limit is defined here as 3 times the standard deviation of baseline counts when the aspirated solution contains no metal divided by the detection sensitivity. The standard deviation in the number of baseline counts is determined by the computer program from data like that shown in Figure 2.

The results are given in Table 1. The data are compared to the concentration of metal expected in typical flue gas from a coal-fired power plant. Except for arsenic, chromium, mercury, and lead, our detection limits are one to two orders of magnitude above the required level. Chromium detection is already in the required range. The detection limits for arsenic, lead and selenium are especially poor. In the case of arsenic and selenium, the poor detection limits are due to a combination of severely decreased detector sensitivity at the requisite wavelengths (~ 200 nm) and the very high excitation energy of these transitions. To increase the detection sensitivity in future studies, a UV-intensified CCD (ICCD) detector will supplant the current photodiode array. The intensified CCD offers several advantages over the PDA. First, the CCD is a two-dimensional detector as opposed to the linear PDA. The data from the extra spatial dimension can be quickly averaged to increase signal to noise. Second, the intensified array has much higher intrinsic sensitivity than the PDA, especially in the far UV region where selenium and arsenic emit. Saturation of the PDA detector often occurs for the metals aluminum, titanium, and silicon. To avoid saturation of the more sensitive ICCD, a mask will be devised to physically block the array at the wavelengths for these strong emissions. Calibrated neutral density filters can be added to the mask to prevent saturation on any lines of interest.

Table 1

Comparison of Detection Limits with Expected Flue Gas Concentrations

Metal	Experimental Detection Limit*	Flue Gas Composition*
Arsenic	6160	10 - 20
Cadmium	70	1 - 5
Cobaltl	70	4 -10
Chromium	10	20 - 40
Mercury	330	5 - 10
Nickel	430	20 - 40
Lead	1090	15 - 25
Selenium	10,910	70 - 100

* Values are in $\mu g/m^3$.

In addition to the calibration data described above, we have obtained spectra of fly ash in the torch with 100% Ar and a 0.95/0.05 argon/air mixture as the carrier gas. We have observed that diluting the intake air with 95% argon facilitates stable torch operation over operation with 100% air and probably slightly increases the plasma temperature. Both of these effects increase the detection sensitivity and lower detection limits. Representative spectra for the wavelength region from 280 - 420 nm are shown in Figure 4.

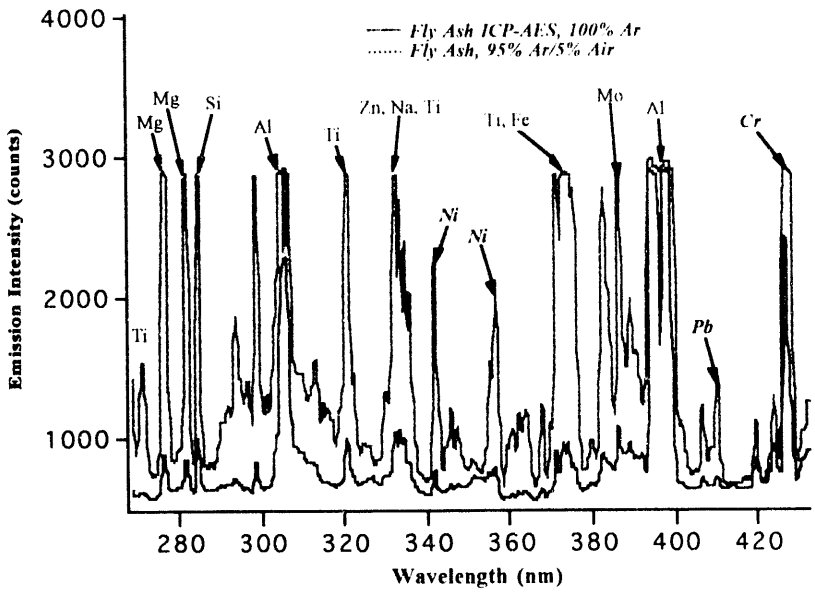

Figure 4: Fly ash ICP-AES spectrum with 100% Ar and a 95/5% Ar/air mixture. CAA metals are denoted by italicized, bold annotation.

Many metals including Si, Mn, Ti, Mg, Al, Zn, Na, Ni, Fe, Mo, Pb, Cr, and Ba can be identified in the fly ash spectra. Of these identifiable metals, Mn, Ni, Pb, and Cr are on the Clean Air Act regulated list, although only Ni, Pb, and Cr are seen in the wavelength range encompassed in Figure 4. An independent assay of this fly ash sample by x-ray fluorescence (XRF) shows that no additional listed toxic metals are present in the sample. The XRF data indicate that Mn, Cr, Ni, and Pb are present in 100, 120, 210, and 40 ppm quantities, respectively. Thus the ICP-AES technique is capable of detecting the regulated metals in actual fly ash samples.

References

1. G.A. Meyer and M.D. Thompson, *Spectrochim. Acta* 40B, 195 (1985).

2. M.D. Seltzer and R.B. Green, Proceedings of the 1990 JANNAF Safety and Environmental Protection Subcommittee Meeting at Lawrence Livermore National Lab, Livermore, CA, held 18 - 22 June 1990.

3. D. Nore, A.M. Gomes, J. Bacri, and J. Cabe, *Spectrochim. Acta* 48B, 1411 (1993).

MERCURY MEASUREMENT AND CONTROL WORKSHOP

Assessment of Mercury Health Risks to Adults from Coal Combustion

F.W. Lipfert, P.D. Moskowitz, V.M. Fthenakis and M. DePhillips
Biomedical and Environmental Assessment Group
Brookhaven National Laboratory
Upton, NY

L. Saroff
Office of Fossil Energy
U.S. Department of Energy
Washington, DC

In the U.S., the general population is exposed to methylmercury (MeHg) principally through the consumption of fish. There is continuing discussion about the sources of this mercury, the magnitude and trends in exposures to consumers, and their health significance. The forums for these discussions extend from the scientific literature to the U.S. Congress. Of special interest because of the health and economic implications associated with its outcome, is the U.S. Environmental Protection Agency study, now scheduled for completion in 1995, which will evaluate the need to regulate mercury emissions from electric utilities. The U.S. Department of Energy, Office of Fossil Energy, is sponsoring a risk assessment project at Brookhaven National Laboratory (BNL) to evaluate independently these same hazards. This report summarizes results from this project (Lipfert et al., 1994).

APPROACH

In this study, health risks to adults associated with mercury emissions from a hypothetical 1000 MW coal-fired power plant were estimated using probabilistic risk assessment techniques. The BNL approach draws on the extant knowledge in each of the important steps in the chain from emissions to health effects. The analysis explicitly recognizes that the general public has a wide range of fish consumption patterns, mainly comprising a variety of species. Further, it is recognized that health effects are keyed to equilibrium levels of Hg body burden, not to the acute effects of individual doses. For this assessment, three separate sources of dietary Hg are defined: canned tuna fish (affected by global Hg), marine shellfish and fin fish (affected by global Hg), and freshwater game fish (affected by both global Hg and local deposition from nearby sources). Wet and dry deposition of Hg from the coal combustion source (a hypothetical power plant) are estimated, and any mercury that is not deposited within 50 km is assumed to enter the global background pool. The incremental Hg in local fish is assumed to be proportional to the incremental total Hg deposition. Existing "reference dose" levels are not used as an index of health effects because of their embedded conservatism; rather, the analysis is based on alternative dose-response models based on the original data on specific neurological responses,

in this case, adult paresthesia (tingling of the extremities). The probabilistic methods used in the assessment specifically incorporate the uncertainties in the dose-response function, as well as in the dose terms.

EMISSIONS AND ATMOSPHERIC PROCESSES

The plant is assumed to burn coal having the U.S. average content of mercury (0.8 ug/g), to be equipped with an electrostatic precipitator, and to have a capacity factor of 75%. Although little reliable data were found on the parameters controlling mercury deposition from power plant plumes, our model compared well with measurements of wet deposition of Hg downwind of an incinerator. There is more information on the relevant atmospheric processes for background Hg, but these data may not apply to the near field (i.e., footprint) of a plume. Results from conventional (short-range) air quality modeling were used, based on the assumption of Gaussian profiles in the power plant plume, to estimate annual air concentrations at the surface, which is assumed to be flat.

Although recent data indicate that a high proportion of mercury in coal-fired power plant stacks is Hg^{++}, there is little or no information on its fate as it travels downwind in the plume. Dry deposition is modeled by assuming a value for the dry deposition velocity (V_d), defined as the ratio of the deposited flux to the air concentration. Different values of V_d are assigned to elemental, water-soluble, and particulate forms of Hg.

Wet deposition was modeled in two different ways, using either the washout ratio (ratio of concentration in precipitation to air concentration) or a dynamic plume depletion model, and similar results were obtained. Both methods require site-specific data on precipitation frequencies, duration, and wind directions. The model suggests that local effects may double or triple the total background deposition of mercury, but that, in any event, about 95% of the Hg emissions from a tall stack will travel beyond the 50 km radius as a result of the low rates of deposition. At this radius, airborne Hg concentrations are reduced drastically, so that the incremental Hg deposition from the plant is of the order of 1% of background levels.

BASELINE MERCURY LEVELS IN SEAFOOD

Substantial variations were found in the mercury concentrations reported for a given fish species. Some of these may be due to differences in laboratory techniques over time and the reporting of total Hg vs. MeHg, but the main sources of variability within a given species are fish size and age, and in addition, for freshwater species, the levels of dissolved organic carbon (DOC) and pH of the water body. It was not possible to identify an effect of watershed/lake surface area ratio on Hg content from existing data, which raises questions as to the mobility of Hg deposited in a watershed. The variations among the average levels of Hg between different fish species were of about the same order as those within a given species, and were probably related to the

trophic level of the fish. When weighted by the quantities caught, there was no difference between average mercury levels in marine shellfish and in marine finfish (both were about 0.1 ug/g), if tunafish are considered separately (which average about 0.2 ug/g). Mercury levels for freshwater game fish were higher (averaging about 0.3 ug/g) and more variable. There was the suggestion of a downward trend in fish Hg concentrations over time, especially for canned tuna, but this could not be confirmed statistically. Better data on mercury levels in seafood are needed. These considerations apply to the baseline status of mercury in seafood, which may include the distributed regional effects of existing coal combustion. To estimate the incremental local effects of a hypothetical plant, proportionality between local mercury deposition from the atmosphere and the mercury content of local fish was assumed. Use of the estimated baseline as a reference point provides a useful "calibration" for the BNL model.

FISH CONSUMPTION RATES AND THE DISTRIBUTION OF BASELINE MeHg DOSES

In order to derive seafood consumption statistics appropriate for this assessment, it was necessary to combine data from various sources. For example, much of the detailed data on distributions of seafood consumption date from 1973-74, and overall consumption has increased substantially since then. Thus, the trend data from national overall production statistics were used to adjust the older distributional statistics upward to more nearly reflect current consumption levels. However, this procedure may entail errors if public preferences for certain species have changed over the years. Good support was found from both surveys and production statistics for an overall average per capita seafood consumption rate of about 25 g/d (about 1 meal per week), with a 95th percentile level of about 80 g/d. About 95% of the U.S. population consumes some seafood over the course of a year. The average daily (baseline) MeHg dose for consumers of freshwater fish in the upper Midwestern U.S. was estimated to be about 4.6 ug/d. The 99th percentile was about 34 ug/d, which is only about 10% of the U.S. Environmental Protection Agency estimated dose threshold for adult health effects. As discussed above, local increases in mercury deposition are assumed to have proportional effects on the mercury dose to the population (consumption levels are assumed to remain at baseline levels).

THE STEADY-STATE DIET-BLOOD-BODY BURDEN MeHg RELATIONSHIP

Several sources of information were found on the relationship between MeHg in the diet and the levels of Hg reached in blood, which then form the basis for the steady-state body burden of MeHg and for neurological health effects. The most commonly used relationship is based on acute MeHg doses by only 5 subjects and does not present a realistic picture of the uncertainties. Epidemiological approaches to this topic tend to suffer from imprecision as to the dietary doses and to biological half-lives. The half-life, which expresses the differential effect of MeHg uptake and excretion, controls

the magnitude of the response expected from a given rate of daily input, together with body weight. A lognormal representation of half-lives determined on 48 Iraqi MeHg poisoning victims as input to the risk assessment.

A key feature of this assessment is the recognition of the need to account for the effective dose averaging that takes place as equilibrium body burdens of MeHg are reached and maintained. The only way to accumulate a lot of MeHg is to eat fish often, since there are parallel limits to the size of each meal and the Hg content of each fish. This averaging process reduces the variability in MeHg experienced by an individual in the long-term. This may help explain why so few cases of adverse health effects are seen in populations of heavy fish consumers.

DOSE-RESPONSE FUNCTIONS

The central nervous system is the principal target for MeHg, with the potential for effects on sensory, visual, and auditory functions. Low doses may create nonspecific symptoms such as paresthesia, malaise, or blurred vision. Higher doses may bring deafness, loss of coordination when walking, and speech disorders, and, in extreme cases, coma and death. Individuals may vary greatly in their responses.

Data on frequency of adult paresthesia (perhaps the mildest symptom of MeHg poisoning) in 122 Iraqi adults who in 1971-1972 consumed mercury contaminated bread, were used to derive a continuous dose-response function, including the uncertainties in the parameters of the function. Contaminated grain was consumed by 82 of the patients, 40 subjects were considered to be unexposed controls. These data are only available as averages for 7 groups of about 20 individuals, classified according to their estimated intake of MeHg and body burdens. The body burden data were corrected to reflect the (nonequilibrium) levels present at the times that symptoms were first noted. Logistic regressions were used to define alternative dose-response models for various assumed levels of background prevalence of paresthesia. The model that fit the observations best in the region of low dose (which is of primary interest here) was selected for use in the risk assessment, but the uncertainties in its parameters were such that the alternative models were included in its overall envelope. The background prevalence rate for paresthesia used was 2.2%, which corresponds with the rate found independently in an unexposed group of about 1000 Iraqi villagers.

ASSESSMENT OF BASELINE AND INCREMENTAL RISKS FROM A 1000 MW PLANT

The statistical distributions of the Hg content of 3 different seafood categories, their rates of consumption, and number of meals consumed in the time to reach 97% of equilibrium dose were combined to define the distribution of doses. The distribution of equilibrium body burdens was based on the distributions of doses, body weights, and biological half-lives. The distribution of responses was defined by the distribution of doses, after considering the uncertainties in the dose-response function. Power plant contributions to MeHg were modeled by incrementing the Hg concentrations in

freshwater fish only, using a uniform statistical distribution ranging from 50% to 200% increase. The effects of power plant emissions on marine species are assumed to be negligible, since these species are primarily affected by global levels of Hg and the U.S. utility industry contributes only a small fraction of the existing global pool each year. The results predicted a baseline average risk level of about 0.003% (3 chances in 100,000), with an upper 95th percentile risk of 0.012%. When power plant increments were added, the expected average risk level increased to 0.011% with an upper 95th percentile risk of 0.033%. To place these risks in context, in a population of 10,000 heavy fish eaters, one case of paresthesia due to fish consumption would be expected in the absence of a power plant, 3 cases with the plant, and about 220 cases due to other causes. If a deterministic hockey-stick dose-response model had been used, the incremental frequency of paresthesia would have been zero in all cases. The effects of emissions of a single power plant on global mercury levels are thus seen to be small in the context of existing background, and this is probably the case for the entire U.S. utility industry as well. However, in the long-term it may be necessary to consider the slow increase in Hg in the global pools. These findings are consistent with the failure of several epidemiological studies to find definitive symptoms of Hg poisoning among populations with heavy fish consumption patterns.

RECOMMENDATIONS

It is clear that the risks of adult paresthesia from fish consumption are low. This analytical framework should be extended to the case of maternal fish consumption and fetal effects on child development, which are thought to be considerably more sensitive. It is also clear that the basic data used in this analysis are in need of improvement:

1. Mercury levels in fish are based on conflicting and outdated data.

2. Fish consumption patterns of sensitive subpopulations (such as pregnant women) have not been established.

3. Appropriate methods for estimating Hg deposition from power plants have not been validated in the field.

4. The intersections of the sets of locations of U.S. coal-fired power plants, sensitive water bodies, and susceptible subpopulations have not been established.

5. Annual total Hg emissions from coal burning and from other sources, including natural sources, are still uncertain, which makes it difficult to estimate the effects of U.S. coal burning on global Hg concentration levels.

6. Since the uncertainty in the dose-response data contributed over half of the variability in the estimates of paresthesia frequency, improved data on health effects should result in substantially more precise assessments.

REFERENCES

Lipfert F.W., P. Moskowitz, V.M. Fthenakis, M. DePhillips, J. Viren and L. Saroff, 1994. Assessment of Mercury Health Risks to Adults from Coal Combustion. BNL Report (in press), Brookhaven National Laboratory, Upton, NY.

EVALUATION OF SORBENTS FOR ENHANCED MERCURY CONTROL

DENNIS L. LAUDAL
STANLEY J. MILLER
ENERGY & ENVIRONMENTAL RESEARCH CENTER
UNIVERSITY OF NORTH DAKOTA
PO BOX 9018
GRAND FORKS, ND 58202-9018

1.0 INTRODUCTION

The ability to remove mercury from power plant flue gas may become important because of the Clean Air Act Amendments' requirement that the U.S. Environmental Protection Agency assess the health risks associated with these emissions. One approach for mercury removal, which may be relatively simple to retrofit, is the injection of sorbents, such as activated carbon, upstream of existing particulate control devices. Activated carbon has been reported to capture mercury when injected into flue gas upstream of a spray dryer baghouse system applied to waste incinerators or coal-fired boilers.[1,2] However, the mercury capture ability of activated carbon injected upstream of an electrostatic precipitator (ESP) or baghouse operated at temperatures between 125° and 175°C is not well known.

A study sponsored by the U.S. Department of Energy and the Electric Power Research Institute is being conducted at the University of North Dakota Energy & Environmental Research Center (EERC) to evaluate whether mercury control with sorbents can be a cost-effective approach for large power plants. Initial results from the study are reported in this paper. Variables of interest include coal type, sorbent type, sorbent addition rate, and temperature.

2.0 EXPERIMENTAL APPROACH

Baseline and sorbent screening tests were conducted at the EERC with a pulverized coal (pc)-fired combustor known as the particulate test combustor (PTC) and a pulse-jet baghouse. Originally, the PTC used cold-water annular heat exchangers to provide flue gas temperature control to the baghouse. However, analysis of ash deposits collected from the heat exchangers indicated that some mercury was collected on the duct walls. To minimize this effect, the heat exchangers were modified for these tests to provide for higher duct wall temperatures. A complete description of the PTC and baghouse was given in a previous report[3].

The tests were conducted with two coals. The first was a Powder River Basin subbituminous coal from the Absaloka mine. The second coal selected was a bituminous coal from the Pittsburgh No. 8 seam, Blacksville mine. Since the level of mercury in the two coals averaged 59 and 85 ppm, respectively, and the coal feed rate to the combustor is about 23 kg/hr, the required sorbent add rate is only about 2 g/hr to achieve a sorbent-to-mercury ratio of 1000. Steady sorbent injection at the required low feed rate was accomplished by using a Model 3410 Dry Powder Disperser (DPD), manufactured by TSI Inc. This instrument is designed to disperse dry bulk powders into their original particle-size distribution in a carrier gas, with precise control over the feed rate. For all sorbent tests, the additive was injected with the DPD into the flue gas duct just upstream of the baghouse.

The purpose of using a dry powder additive injected just upstream of an ESP or fabric filter is to retain the vapor-phase mercury by either physical absorption or chemical bonding. The dry additive is then collected in the fabric filter or ESP along with the fly ash. An ideal additive should have the following attributes:

- Be a good mercury sorbent both in terms of the level of control achieved and the amount of additive needed

- Be effective over a broad temperature range
- Not be considered a hazardous waste
- Not readily release the collected mercury upon exposure to water and/or air
- Not adversely affect the performance of the ESP or fabric filter
- Be reasonable in cost

Carbon-based sorbents have been shown to be effective for controlling vapor-phase trace elements, especially mercury, in a number of applications, including waste incineration and natural gas production.[2,4] However, until recently little research examined activated carbon sorbents in coal combustion systems. Activated carbon can be made from a number of different sources, including wood, coal, bone, and coconut shells. Two primary types tested for control of mercury in waste incinerators are made from either lignite or wood. Lignite char is thermally activated using steam, while wood char is chemically activated. Either activated carbon can be used in an unadulterated state, where absorption of the vapor-phase mercury is the dominant mechanism, or the carbon can be impregnated with sulfur, iodine, or compounds of these elements. The mercury then reacts with the sulfur or iodine to enhance mercury retention in the particulate control device. Two carbon-based sorbents used in this study included a lignite-based activated carbon, which is commercially available from American Norit Co, inc., and an activated carbon impregnated with an iodine compound, which is commercially available from Barnebey & Sutcliffe Corp.

Simultaneous inlet and outlet mercury sampling was conducted according to tentative EPA Method 29, also known as a multimetal sampling train method. Method 29 does not claim to speciate between oxidized and elemental mercury, but other researchers have indicated that oxidized mercury will be trapped in the peroxide impingers and elemental mercury in the permanganate impingers.[5,6] To further evaluate the mercury speciation ability of Method 29, bench-scale tests were conducted in which mercury(II) chloride ($HgCl_2$)and elemental mercury permeation tubes were used as known mercury sources.

Mercury analyses were completed with a Leeman PS200 cold-vapor atomic adsorption (CVAA) analyzer. To ensure precision and accuracy, the instrument was calibrated on a regular basis using quality control standards.

3.0 RESULTS AND DISCUSSION

3.1 Coal Analysis

Two of the coal characteristics important to the selection process were the mercury content and chlorine content. The average mercury concentration on a dry basis for the Absaloka coal was 59 ppb, with a standard deviation of 10 ppb for 11 samples. The mercury content of the Blacksville bituminous coal was 98 ppb, with a standard deviation of 17 ppb on a dry basis for six samples. On a dry coal mass basis, the bituminous coal had a significantly higher mercury concentration, but on a constant heating value basis, the difference is not as great.

It has been reported that the concentration of chlorine in coal is important in determining the species of mercury emitted in the flue gas.[2] A higher level of chlorine in the coal is expected to increase the fraction of mercury that is emitted as $HgCl_2$. The chlorine concentration in the Blacksville coal was about 18 times greater than in the Absaloka coal, 790 ppm, as compared to 45 ppm.

3.2 Bench-Scale Method 29 Mercury Speciation Tests

Tests were conducted in which nitrogen was passed over elemental mercury and $HgCl_2$ permeation tubes. In the case of elemental mercury, nine tests with mercury concentrations ranging from 10 to 100 $\mu g/m^3$ all showed that at least 99% of the mercury was collected in the permanganate impingers and 1% or less collected in the peroxide impingers. Nine tests with $HgCl_2$ indicated that most of the oxidized mercury is retained in the hydrogen peroxide impingers, but some small amount appears to penetrate and is detected in the permanganate impingers. Results indicate that the percentage of the oxidized mercury that is collected in the peroxide is somewhat dependent upon the mercury concentration. At $HgCl_2$ concentrations greater than 20 $\mu g/m^3$, more than 99% is retained in the peroxide, but the percentage retained appears to be slightly reduced at lower concentrations. The data indicate that in the range of 5 to 10 $\mu g/m^3$, which is typical of inlet mercury concentrations from coal combustion, more than 96% is retained in the peroxide. This level of retention should provide adequate speciation of the oxidized mercury. These data indicate that Method 29 can adequately speciate between elemental mercury and $HgCl_2$. However, the results do not prove that other forms of oxidized mercury will be correctly speciated by the method.

Bench-scale sorbent screening tests were also conducted using lignite-based and iodine-impregnated activated carbons and simulated flue gas. The simulated flue gas was 3.5% oxygen, 10% carbon dioxide and water vapor, with the balance nitrogen. No sulfur dioxide or chlorine was added for these tests. A 645 cm^2 Ryton fabric, held in a heated stainless steel holder, was used to collected the sorbent and fly ash. The sorbent was premixed with fly ash to achieve the desired sorbent-to-mercury mass ratio and injected by DPD upstream of the filter. The fly ash selected for these tests was pulse-jet baghouse hopper ash from baseline tests firing the Absaloka subbituminous coal. As in the previous bench-scale tests, the elemental mercury and $HgCl_2$ were obtained using permeation tubes. For all tests, it was apparent that the stainless steel filter holder converted oxidized mercury to elemental mercury at the temperatures tested (93° and 149°C). Because of the conversion that occurred, it was difficult to interpret the data; however, the data appear to confirm preliminary conclusions from the combustion tests that the iodine-impregnated activated carbon is an effective sorbent for the elemental mercury. Because of the conversion of oxidized to elemental mercury, no conclusion could be made for the lignite-based activated carbon tests. For future bench-scale tests, the filter holder and all other exposed stainless steel tubes, fittings, and connections will be coated with teflon.

3.3 Combustion Tests

The inlet sampling location was upstream from the sorbent injection port, which allowed combining the inlet data for each coal. Average inlet mercury data for the Absaloka coal are shown in Figure 1 and for the Blacksville coal in Figure 2. The total mercury measured by Method 29 includes mercury retained on the filter, mercury collected in the peroxide impingers (considered to be oxidized mercury), and the mercury collected in the permanganate impingers (considered to be elemental mercury). Total inlet mercury concentrations for each coal were fairly constant from test to test as indicated by the error bars, which represent plus or minus one standard deviation.

For the Absaloka coal, a significant amount of mercury was retained on the filter, ranging from 80% at 125°C to 26% at 200°C. The filter temperature of the Method 29 train was adjusted to the same temperature as the baghouse for each test. In general, the amount of mercury retained by the particulate matter on the inlet sampling filter was consistent with the mercury retained in the baghouse hopper ash for the tests without sorbent injection. This is not surprising, since both were at the same temperature and both the sampling filter and baghouse are good gas-solid contactors. The fact that the same approximate concentrations show up in the inlet filter and baghouse hopper ash is an indication that the analyses are correct.

From Figures 1 and 2, significant differences are apparent between the mercury speciation for the two coals. Oxidized mercury for the Absaloka tests was less than 1 $\mu g/m^3$, while it ranged from 3.7 to

5.4 $\mu g/m^3$ for the bituminous coal. Elemental mercury was less than 0.5 $\mu g/m^3$ and did not appear to be temperature-dependent for the Blacksville tests; it ranged from 0.8 to 3.7 $\mu g/m^3$ for the Absaloka coal, increasing significantly with temperature. For both coals, the filter mercury decreased with increasing temperature, but the fraction of the total mercury retained on the filter was much lower with the Blacksville coal. One factor thought to influence the amount of mercury retained in fly ash is the loss on ignition (LOI), which indicates the amount of unburned carbon in the ash. Higher LOI is expected to result in higher mercury retention, because the unburned carbon may behave similarly to carbon-based sorbents. However, these results seem to contradict that suggestion in that the fly ash LOI was low for the baseline Absaloka tests (0.4%-0.7%) and high for the baseline Blacksville tests (4%-13%). LOI may influence the amount of retained mercury for a given coal, but, evidently, other factors may override the LOI effect when various coals are compared. The results also appear to refute the common observation that oxidized mercury is more readily retained on the fly ash, since greater mercury retention was observed with the Absaloka coal, which had the lower oxidized mercury level. However, the form of mercury retained by the filter or baghouse is not known; Method 29 provides speciation information for the vapor-phase mercury only.

The data indicate a difference in mercury retention by the fly ash that is related to coal type, but the cause is not clear. Since the Absaloka coal is very low in chlorine, perhaps other mercury species such as mercury(II) oxide (HgO) could form. HgO has a much lower vapor pressure than $HgCl_2$ or elemental mercury and might be more readily retained by the ash at a higher temperature. Another possibility is that, even though the LOI of the fly ash was low for the Absaloka runs, enough unburned carbon of a type that is a good mercury sorbent may be available in the fly ash to retain mercury. Why this might occur for the Absaloka tests and not the Blacksville tests is not clear. A third explanation is that some other species, such as high surface area calcium or magnesium compounds, are present in the Absaloka fly ash to enhance mercury retention. These species might not form with the Blacksville coal, which is much lower in calcium and magnesium.

Baseline tests without sorbent addition and tests in which lignite-based activated carbon and iodine-impregnated activated carbon were injected just upstream of the baghouse were conducted with the pilot combustion system. Most tests were completed over a continuous two-day period and included four pairs of simultaneous inlet-outlet Method 29 measurements. The mercury removal results for the Absaloka and Blacksville tests are shown in Figures 3 and 4. Values reported are based on the total inlet and total outlet mercury concentration. The error bars shown represent plus or minus one standard deviation. Total mercury for both inlet and outlet included filter mercury, oxidized mercury, and elemental mercury. However, the baghouse particulate collection efficiency was typically about 99.99%, so very little fly ash was collected on the outlet sampling filter. In all cases, any mercury collected on the outlet filter was below detection limits, so the total measured outlet mercury consisted only of vapor-phase oxidized and elemental mercury.

For the Absaloka baseline tests, the total mercury removal across the baghouse was highly temperature-dependent, ranging from 80% at 125°C to 30% at 200°C. Note that the baseline mercury removal across the baghouse is in good agreement with the inlet mercury retained on the sampling filter, even though they are based on independent measurements. With the Blacksville coal, baseline mercury removal was much lower, ranging from 30% at 120°C to 3% at 175°C.

Lignite-based activated carbon was injected into the flue gas at sorbent-to-mercury mass ratios of approximately 3000:1 and 9400:1, and the iodine-impregnated activated carbon was injected at a ratio of 1000:1. Preliminary screening tests indicated that a ratio of 1000:1 for the lignite-based carbon did not provide significant control, so the ratio was increased to 3000:1. Preliminary tests indicated that a ratio of 1000:1 with the iodine-impregnated carbon provided adequate mercury control, so the ratio was not increased in subsequent tests. From Figure 3, data indicate the Absaloka tests the lignite-based activated carbon provided some improvement in mercury capture over the baseline condition. However, the lignite-based carbon removed only about half of the remaining mercury that was not removed naturally. If there were little natural mercury removal, the lignite-based activated carbon may not provide

any better than 50% control at these temperatures and this add rate. The iodine-impregnated activated carbon provided much better control and was effective at both 150° and 200°C. The outlet Method 29 data indicate that the iodine-impregnated carbon collected about 95% of the elemental mercury and 45% of the oxidized mercury. This suggests that iodine-impregnated activated carbon is an effective mercury sorbent when most of the mercury is in elemental form.

Results from the Blacksville tests, shown in Figure 4, indicate that lignite-based activated carbon will provide good mercury control at 93°C (97%), but the mercury removal deteriorates significantly as the temperature is increased. Increasing the sorbent-to-mercury mass ratio to 9400:1 had little impact on the mercury collection efficiency. The iodine-impregnated carbon provided somewhat better control than the lignite-based carbon at 125°C, but little mercury removal was observed at 175°C. These results differ from the iodine-impregnated carbon results with the Absaloka coal that showed excellent mercury removal in the range from 150° to 200°C. However, the results can be explained by considering the inlet mercury speciation. The vapor-phase mercury with Absaloka coal was predominately elemental, while very little of the vapor-phase mercury with Blacksville coal was elemental. The Method 29 outlet measurements indicate that the iodine-impregnated activated carbon removed almost all of the elemental mercury at both temperatures for the Blacksville tests, but, since the amount of elemental mercury was small, the effect on total mercury removal was minimal. The iodine-impregnated activated carbon was somewhat effective at removing oxidized mercury species at 125°C, while very little oxidized mercury removal was seen at 175°C. Therefore, data indicate that the ability of the iodine-impregnated activated carbon to capture oxidized mercury is highly temperature-dependent, but the ability to capture elemental mercury species is less temperature-dependent (at least within the temperature range examined). To achieve a higher overall mercury vapor removal when a significant portion of the mercury is in oxidized form, higher sorbent feed rates and/or a lower temperature are needed. The mercury removal data at 175°C with the Blacksville coal are of concern because neither the lignite-based nor iodine-impregnated activated carbons provided effective mercury control when most of the mercury was in oxidized form. Whether improved mercury control can be achieved at 175°C by substantially increasing the sorbent addition rates is unknown.

4.0 PRELIMINARY CONCLUSIONS

- Method 29 appears to adequately speciate between $HgCl_2$ and elemental mercury.
- Stainless steel appears to convert $HgCl_2$ to elemental mercury in bench-scale tests using simulated flue gas at the temperatures tested.
- Inlet mercury speciation for the Absaloka subbituminous and Blacksville bituminous coals was significantly different.
- With the subbituminous coal, significant amounts of mercury were retained by the particulate matter collected on the inlet sampling filter and the baghouse hopper ash at lower temperatures.
- Less mercury was retained in the baghouse hopper ash with the bituminous coal even though the oxidized mercury and LOI were much higher.
- Iodine-impregnated activated carbon provided effective mercury control at 150° and 200°C with the subbituminous coal.
- Iodine-impregnated activated carbon was highly effective at removing elemental mercury for both coals.

- Iodine-impregnated activated carbon provided some removal of oxidized mercury at lower temperatures.

- Lignite-based activated carbon provided some mercury control at lower temperatures.

5.0 REFERENCES

1. Felsvang, K.; Gleieser, R.; Juip, G.; et al. "Air Toxics Control by Spray Dryer Absorption Systems," Presented at the 2nd International Conference on Managing Hazardous Air Pollutants, Washington, 1993.

2. White, D.M.; Nebel, K.L.; Brna, T.G.; et al. "Parametric Evaluation of Powdered Activated Carbon Injection for Control of Mercury Emissions from a Municipal Waste Combustor," Presented at the 85th Annual Meeting of the Air & Waste Management Association, Paper No. 92-40.06, Kansas City, 1992.

3. Miller, S.J.; Laudal, D.L. "Pulse-Jet Baghouse Performance Improvement with Flue Gas Conditioning," final project report for Project No. RP-3083-9 for Electric Power Research Institute, U.S. Department of Energy, and Canadian Electric Association; October, 1992.

4. Biscan, D.A.; Gebhard, R.S.; Matviya, T.M. "Impact of Process Conditions on Mercury Removal from Natural Gas Using Activated Carbon," *In* Proceedings of the 8th International Conference on Liquefied Natural Gas; 1986, pp 1-12.

5. Tumati, P.R.; DeVito, M.S. "Partitioning Behavior During Coal Combustion," Presented at the Joint ASME/IEEE Power Generation Conference, Paper No. 93-JPGC-EC-8, Kansas City, 1993.

6. Chang, R.; Bustard, C.J.; Shott, G.; et al. "Pilot Scale Evaluation of Activated Carbon for the Removal of Mercury at Coal-fired Utility Power Plants," Presented at the 2nd International Conference on Managing Hazardous Air Pollutants, Washington, 1993.

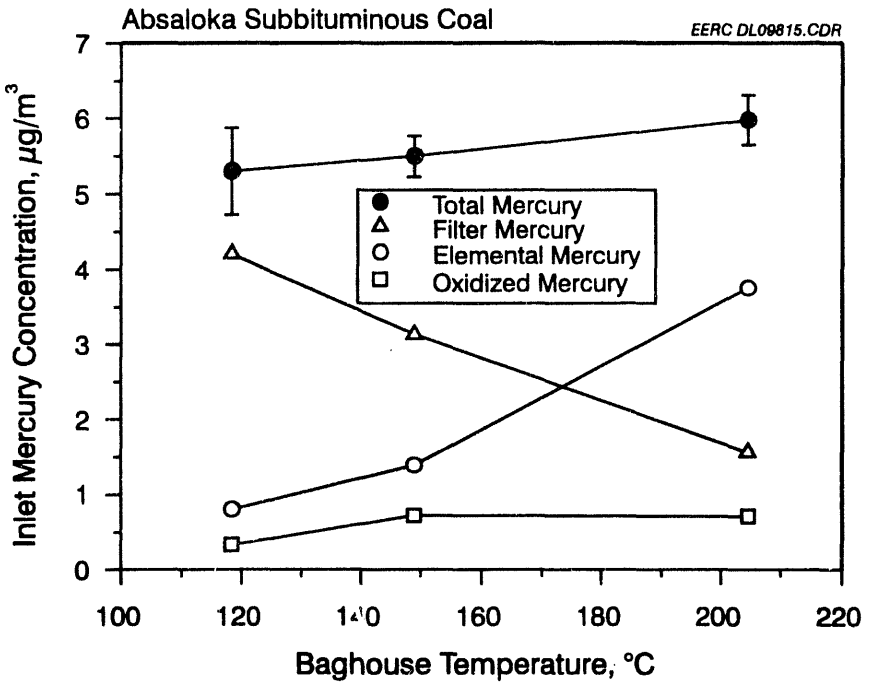

Figure 1. Average inlet mercury concentrations for Absaloka subbituminous coal. Error bars represent plus and minus one standard deviation.

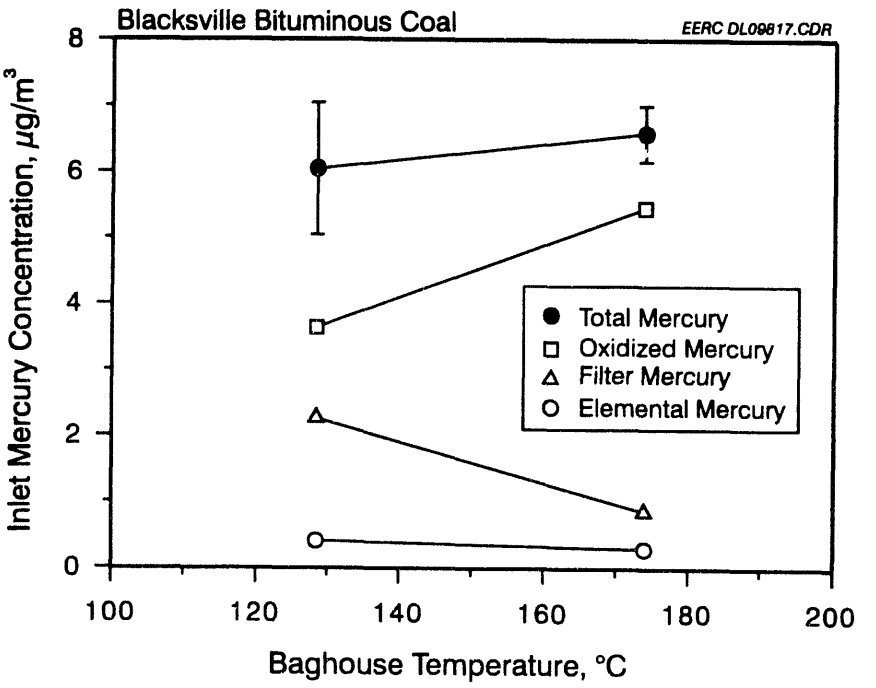

Figure 2. Average inlet mercury concentrations for Blacksville bituminous coal. Error bars represent plus and minus one standard deviation.

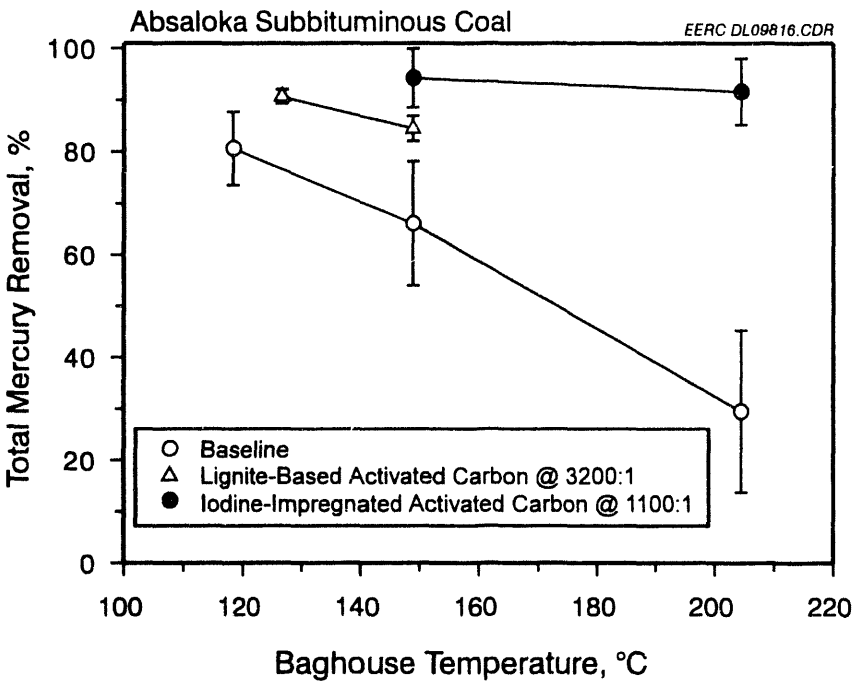

Figure 3. Total mercury removal across the baghouse for Absaloka subbituminous coal. Error bars represent plus and minus one standard deviation.

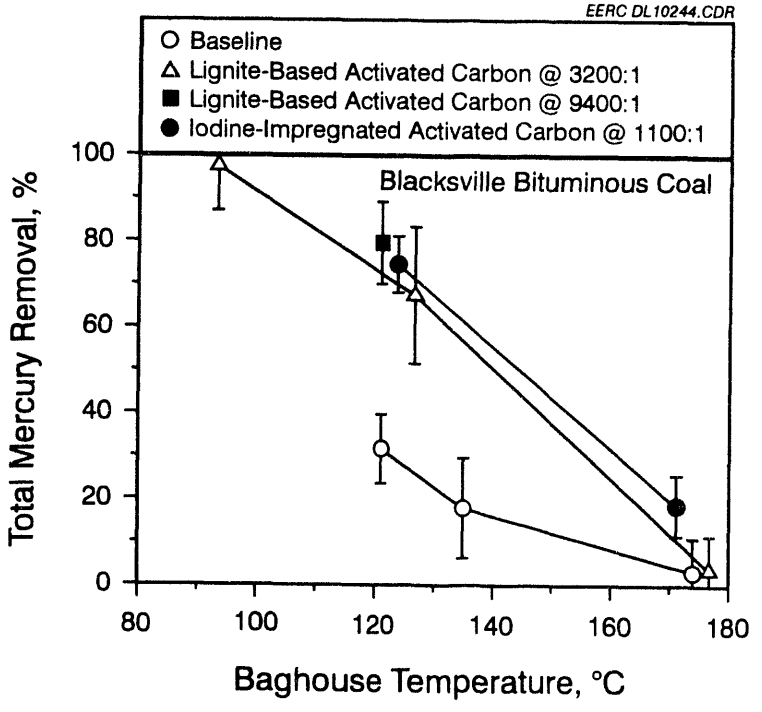

Figure 4. Total mercury removal across the baghouse for Blacksville bituminous coal. Error bars represent plus and minus one standard deviation.

The following manuscript was unavailable at the time of publication.

MERCURY CAPTURE FROM A BENCH-SCALE SCRUBBER

D. Livengood
Argonne National Laboratory
9700 S. Cass Avenue
Argonne, IL 60439

Please contact author(s) for a copy of this paper.

The following manuscript was unavailable at the time of publication.

EVOLUTION OF THE SAMPLING AND ANALYTICAL METHODS FOR DETERMINING TOTAL AND SPECIATED FORMS OF MERCURY

B. Nott
EPRI
3412 Hillview Avenue
P.O. Box 10412
Palo Alto, CA 94303

Please contact author(s) for a copy of this paper.

MEASUREMENT OF MERCURY AND OTHER TRACE METALS IN COMBUSTION GASES USING ACTIVE NITROGEN ENERGY TRANSFER (ANET)

L.G. PIPER, H. DU, M.E. FRASER, S.J. DAVIS, PHYSICAL SCIENCES INC,
20 NEW ENGLAND BUSINESS CENTER, ANDOVER, MA, 01810-1022

ABSTRACT

We describe an innovative technique to detect mercury at sub part-per-billion levels. Our approach exploits active nitrogen energy-transfer (ANET) excitation of atomic fluorescence. ANET excitation populates only one emission line of mercury at 253.7 nm. This means that the ANET spectrum can be analyzed with instrumentation of modest resolution.

We use dielectric-barrier (D-B) discharge technology to generate the active nitrogen. This approach affords atmospheric-pressure operation, can excite fluorescence in gaseous, particulate, and aqueous sample matrices, and is amenable to field operation because the discharge and associated electronics can be powered by 12V batteries.

This paper describes the results of a laboratory investigation that demonstrates detection of elemental mercury both in the gas phase and on particulates. In addition we show that mercuric chloride can be detected sensitively and can be differentiated from elemental mercury. Our results indicate sensitivity limits below 100 parts per trillion in the presence of simulated flue gas.

1. INTRODUCTION

Mercury is the most significant toxic heavy-metal effluent from coal-burning power plants. Because power plants typically burn more than 1,000 tons of coal each day, even small concentrations of mercury in the coal, on the order of 0.1 to 1 parts per million by weight (ppmw), could result in the introduction of more than a ton of mercury into the environment each year unless the mercury is scrubbed from the exhaust stack. Verifying the effectiveness of the scrubbing process requires on-line, real-time monitoring of mercury concentrations in the power plant exhaust.

We are in the process of developing a compact, portable instrument that will allow real-time, *in situ* monitoring of mercury levels in power plant flue gases. Our instrument will indicate whether or not clean-up technologies are successful at reducing mercury emissions below regulated levels, and will provide feedback to allow changes in operating conditions, if necessary, to bring emissions back into environmental compliance.

Our technique, discussed in more detail below, is to excite mercury fluorescence at 253.7 nm by the technique of active nitrogen energy transfer (ANET). The active nitrogen is made in a dielectric-barrier (D-B) discharge operating in nitrogen at atmospheric pressure. Only the one line of mercury is excited, so spectral resolution requirements are greatly simplified over those of other spectroscopic techniques. The dielectric-barrier discharge is quite compact, 1 to 2 cm in diameter and 1 to 10 cm long. Furthermore, the discharge power requirements are quite modest, so that the unit can be powered by batteries. Thus an instrument based on ANET can readily be made portable. Finally, ANET has the ability to differentiate free mercury from $HgCl_2$ by exciting emission from HgCl around 540 nm.

This paper reports preliminary results from our study of the excitation of Hg in a D-B discharge in N_2 at atmospheric pressure. We have determined the overall sensitivity of Hg detection in the presence of gas whose composition is representative of that found in flue gas in coal-burning power plants. In addition, we demonstrate that ANET can be used to differentiate between elemental mercury and mercuric chloride, and that ANET can detect the presence of mercury on particulates.

2. BACKGROUND MATERIAL

2.1 *Active Nitrogen Energy Transfer (ANET)*

From the beginning of this century, scientists have observed characteristic emissions from atoms and free radicals when atomic and molecular species were added to active nitrogen. A rich literature exists detailing the chemical reactions and energy-transfer processes that occur to excite these emissions.[1-4] Basically, metastable nitrogen molecules in the active nitrogen transfer their energy to the various acceptor species. These acceptor species then fluoresce at wavelengths characteristic of the acceptor. Generally metastable nitrogen excites only

a small number of states of the acceptor species so that the ANET-induced fluorescence is relatively simple and uncomplicated. Most metastable nitrogen energy transfer processes are quite efficient, generally occurring at rates on the order of one-tenth gas kinetic or greater.[5] As a result ANET fluorescence can be quite strong.

Most studies on processes occurring in active nitrogen relied upon the recombination of nitrogen atoms at relatively low pressures to generate the metastable nitrogen molecules. For analytical applications, this approach has the disadvantage that considerable power is required to dissociate atomic nitrogen. In addition, because these systems operate at pressures on the order of 1 to 10 Torr, a vacuum system is required.

We conceived and began developing ANET as an alternative to active nitrogen analytical techniques relying on atomic-nitrogen recombination as the active nitrogen source. Our approach is to generate the metastables in a dielectric-barrier discharge operating at atmospheric pressure and total power less than 2 Watts. Thus, our system requires neither a large power source nor a vacuum system. In addition, our observations indicate that the overall metastable number densities generated in the dielectric-barrier discharge are several orders of magnitude larger than those in the atom-recombination system, which means that ANET has the potential to be several orders of magnitude more sensitive.

2.2 Dielectric-Barrier Discharge Technology

A dielectric-barrier discharge is a high voltage a.c. discharge between two electrodes, at least one of which is separated from the discharge region by a dielectric barrier (insulator) such as glass[6,7] (see Fig. 1). A typical discharge will run at voltages between 3 and 30 kV at frequencies from line frequency to 100 kHz. Gas pressures are typically an atmosphere and gap spacings are on the order of a few millimeters. In its simplest form, the discharge can be powered by attaching the electrodes to the output of a high voltage, step-up transformer, such as a neon-sign transformer, plugged into a variac.

The dielectric-barrier discharge is often referred to as an ozonizer discharge because it is the discharge used in efficient commercial ozone generators. It is not a single discharge in the sense of a continuous arc or glow discharge, but rather a dense collection of microdischarges between the dielectric and the other electrode. These microdischarges consist of short duration (typically 10 to 100 ns) current pulses (100 to 1000 A cm^{-2}) localized in roughly cylindrical filaments, typically 100 μm in radius. Although the current *densities* in the microdischarges are quite large, the overall power consumption of a typical dielectric-barrier discharge is relatively modest. Often the total current drain will be only a few milliamps, resulting in an overall power consumption on the order of 10 Watts.

The mean electron energy in the microdischarge is on the order of 1 to 10 eV and can be varied by changing the gas pressure and interelectrode gap spacing. Thus one can tune the electron energy of the discharge to selectively enhance the excitation of one species over another. At any given instant in time, the microdischarges are distributed uniformly across the face of the dielectric. This uniformity provides a relatively stable excitation throughout the discharge volume.

The energy in a typical microdischarge, 10 kV, 300 A cm^{-2}, 10 ns duration, and 100 μm radius, is about 10 μJ. This is more than enough energy to vaporize small particles in the discharge region if a microdischarge terminates on them. The minimum energy required to vaporize a dust particle will be equal to the heat necessary to raise the particle temperature to its vaporization point plus the particle's the latent heat of vaporization. For a particle of SiO_2, the total energy required to achieve complete vaporization will be about 600 kJ $mole^{-1}$. Thus for a typical particle of size 1μm radius and density of about 2.5 g cm^{-3}, we calculate that the energy required for complete vaporization is about 0.2 μJ, much less than the energy of a single micro-discharge. The resultant vapor can then interact with the active nitrogen and induce it to fluoresce.

2.3 The Chemistry and Physics of ANET

Dielectric-barrier discharges in pure nitrogen have been shown to be efficient sources of metastable $N_2(A^3\Sigma_u^+)$[8-10], even at pressures of one atmosphere, thus providing the active nitrogen source necessary to the selective analyte excitation of ANET. If the analyte species is free mercury, the excitation occurs directly. When molecular species are added to the discharge region, the $N_2(A)$ generally reacts with the molecule, producing molecular fragments, which it subsequently excites. For example, $HgCl_2$ is dissociated to HgCl whose emission is readily observed near 540 nm.

The chemical processes responsible for exciting fluorescence from Hg in a dielectric-barrier discharge are summarized by the following reactions:

$$N_2 + e^- \rightarrow N_2^* + e^- \quad (1)$$
$$N_2^* + N_2 \rightarrow N_2 + N_2 \quad (2)$$
$$N_2^* + Hg \rightarrow Hg^* + N_2(X) \quad (3)$$
$$Hg^* \rightarrow Hg + h\upsilon \text{ (wavelength = 253.7 nm)} \quad (4)$$
$$Hg^* + N_2 \rightarrow Hg + N_2 \quad (5)$$
$$Hg^* + Q \rightarrow Hg + Q' \quad (6)$$
$$N_2^* + Q \rightarrow N_2 + Q', \quad (7)$$

where, Q represents a species in the discharge that quenches electronic energy in either the N_2^* or the electronically excited mercury.

Although the dielectric-barrier discharge is a pulsed discharge, one can treat it as if it were a continuous discharge if observations are averaged over a number of discharge cycles. Then, because of their short radiative and quenching lifetimes, the excited species in the discharge region are effectively in steady state and we can write

$$I_{Hg^*} = k_4[Hg^*] = k_3[Hg][N_2^*]/(1 + (k_5/k_4)[N_2] + (k_6/k_4)[Q]) . \quad (8)$$

Equation (8) shows that for constant metastable number density and total pressure, the fluorescence intensity will be linearly proportional to the additive number density, provided the number densities of any potential quenchers remain constant. This generally will be the case. The linearity of active-nitrogen excited fluorescence intensity with analyte number density has been demonstrated experimentally to cover four to five orders of magnitude for a number of species.

The exciting species in active nitrogen generally is considered to be $N_2(A\ ^3\Sigma_u^+)$, although other nitrogen metastables can also contribute. $N_2(A)$ carries about 6 eV of internal energy. Based on the reaction scheme above, its steady state number density is given by

$$[N_2^*] = k_1[e^-][N_2]/(k_2[N_2] + k_3[Hg] + k_7[Q]) . \quad (9)$$

The radiative lifetime[11] of $N_2(A)$ is about 2.5s. Thus, the primary mechanism for its deactivation will be quenching rather than radiative decay.

Quenching of either the mercury fluorescence or the nitrogen metastables can be an issue affecting the sensitivity of ANET. Although rate coefficients for quenching mercury 253.7 nm emission and $N_2(A\ ^3\Sigma_u^+)$ are known for a number of important species[5,12-14], we prefer to determine the effects of quenching *in situ* to ensure that unexpected processes do not complicate our analysis. We have made a number of observations related to metastable nitrogen quenching in the D-B discharge[15], and have obtained results consistent with more direct quenching measurements. Mercury fluorescence quenching, in the presence of oxygen, is more complex than the simple model shown above. However, but as we show below, it does not seriously compromise the overall sensitivity of the ANET technique.

3. EXPERIMENTAL

The bulk of our experiments, were done in the laboratory to demonstrate feasibility of using ANET for mercury detection. This effort used the apparatus shown schematically in Fig.2. It consists of a dielectric-barrier discharge lamp, power source, optical multichannel analyzer, and gas handling lines.

We have constructed lamps in both planar and annular geometries[16] using a variety of dielectrics, including Pyrex, quartz, alumina, and sapphire. Most of our experiments used models similar to that shown schematically in Fig. 1 above. It is fabricated from a single piece of quartz having a 12 mm o.d. body with an axial protrusion inside the 12 mm tube. We used several lamps with various protrusion diameters ranging from 3 to 8 mm o.d. The end opposite the protrusion is sealed with a quartz window. Gas enters the lamp through a side arm situated at the end of the lamp nearest the window and exits through another side arm at the opposite end of the lamp body. The general flow of gas away from the window helps maintain a cleaner environment in the discharge region and keeps the window free from the build up of contamination.

The lamp has an annular discharge region. The outer electrode is formed by wrapping copper-foil tape around the outside of the lamp body. The inner electrode is formed by painting the inside of the axial

protrusion with a layer of conductive material such as graphite, nickel or silver. A wire, wrapped loosely with copper turnings to contact the conductive inner surface, is inserted into the protrusion and is connected to the power supply. This configuration provides a clean discharge region since all surfaces are quartz.

Our power source was the output of a 15 kV neon sign transformer with a center-tap-grounded secondary winding. The voltage to the primary is controlled by a variac operating off standard 60 Hz ac power. For a few measurements we connected the electrodes to the secondary of an automotive ignition coil which was powered with 12 V square-wave pulses at frequencies between 45 Hz and 3 kHz. This power source has great potential because it lends itself to battery operation.[16]

Elemental mercury or mercuric chloride powder was placed in a cold finger immersed in a bath that was thermostated for vapor pressure control. A small flow of nitrogen through the cold finger transported the sample vapor into the discharge region. The concentration of the analyte in the discharge region was equal the product of the compound's vapor pressure in the cold finger and the dilution factor between the N_2 flow through the cold finger and that through the D-B lamp as a whole. Because elemental mercury is so readily detected by ANET, the temperature of the thermostated bath was kept quite cold. In many experiments we used a $CHCl_3$ slush bath to maintain a temperature of -63 ^{o}C. At this temperature, the vapor pressure of mercury is about 2 x 10^{-8} Torr. Slightly warmer temperatures were achieved by making slush baths from mixtures of water and methanol. The bath temperatures were measured with a thermocouple or thermometer.

We found it was important to use Teflon® fittings and tubing in the gas-handling lines exposed to mercury. Mercury has a tendency to permeate most materials including polyethylene, polypropylene, and stainless steel. If these materials are used, they will soak up mercury, and subsequently release it into the gas stream. It then becomes nearly impossible to *avoid* detecting mercury, even when none is intentionally added to the discharge region. In addition, we found that we could maintain a cleaner discharge region when we switched from a Pyrex® lamp to one made from fused quartz.

We used an optical multichannel analyzer (OMA) to detect the fluorescence excited in these experiments. The discharge lamp was placed about 1.5 cm in front of the entrance slit of a 0.32 m monochromator. We generally used a 2400 groove mm^{-1} grating, although a few experiments used gratings with 300 grooves mm^{-1} and 1200 groove mm^{-1}. Dispersed emission spectra were recorded by a Princeton Instruments ST210 Optical Multichannel Analyzer (OMA) system with an intensified linear diode array. The lamp was sufficiently bright, that relatively high resolution spectra ($\Delta\lambda \sim 0.1$ nm) could be accumulated with good signal to noise in only 10 seconds. In some instances longer accumulation times were used. Data were stored in a computer for later analysis.

4. RESULTS

4.1 Detection of Elemental Mercury

Figure 3 shows the spectral region in the vicinity of the Hg 253.7 nm emission line. The mercury line is prominent in the spectrum, and is surrounded, but well separated from, several bands of the NO($A\ ^2\Sigma^+$ -- $X\ ^2\Pi$) system. These bands are also excited by energy transfer from metastable nitrogen[22]. The NO is formed in the discharge in reactions involving traces of oxygen in the nitrogen.

Figure 4 shows how the intensity of the mercury emission varies as a function of the concentration of mercury added to the discharge region. The abscissa refers to concentration in terms of parts per trillion on a volume basis in the discharge region. These data can be used to estimate the sensitivity of the ANET technique. Conditions for these measurements were simplified, only Hg and N_2 were in the lamp. The line through the data points indicates the best linear least-squares fit to the data. The slope of the line is about 1 x 10^7 counts ppb^{-1}. Since a signal of 50 counts is readily observable, we determine a minimum detectability of 5 x 10^{-6} ppb under ideal conditions.

In a practical situation, one is not likely to be able to take samples from a pure nitrogen environment. Thus it becomes important to determine the effects of added species that are likely to accompany the sample. If these species quench the mercury fluorescence, then the sensitivity of ANET will be reduced. To learn about this, we monitored the mercury signal from the D-B lamp as a simulated-flue gas was added to the discharge. We made the simulated-flue gas by flowing a mixture of 5% CO_2, 10% O_2, 85% N_2 through a cell containing water at ambient conditions. The final mixture thus contained about 3% H_2O.

Figure 5 shows the results of adding the simulated-flue gas to a D-B lamp containing a trace of Hg. The Hg signal intensity is plotted in Stern-Volmer fashion, i.e. the reciprocal of the expression in Eq. 8. Such a plot should then be linear in concentration of added quencher if all other conditions remain constant. As can be seen, the added simulated flue gas is quite efficient at quenching the mercury radiation. The half-quenching mole fraction is the added mole fraction of quencher that reduces the signal level by a factor of 2. It can be computed from the ratio of the intercept in the plot in Fig. 5 to the plot's slope. That value is 1.5×10^{-4}.

The results from Figs. 4 and 5 can be combined to determine an effective sensitivity for detecting mercury in the flue gas. That number will be twice the minimum detectable level under ideal conditions divided by the half-quenching mole fraction. We calculate a value of 0.07 ppb. That means that we will be able to detect mercury levels as low as 0.07 ppb in the flue gas even though the sample size is quite small (i.e. about 0.01% of the total gas in the lamp), and in spite of the fact that the flue gas is relatively efficient at quenching the mercury emission.

4.2 Detection of Mercuric Chloride

Adding traces of gaseous mercuric chloride to a D-B discharge in nitrogen results in emission of $HgCl(B^2\Sigma^+ -- X\ ^2\Sigma^+)$, as shown in Fig. 6. The trap containing the $HgCl_2$ was at room temperature, so it's partial pressure in the reagent feed was only 1.3×10^{-4} Torr. Thus, the $HgCl_2$ in the lamp is at sub ppm levels. None-the-less, the spectrum is quite strong and readily assigned. An interesting feature in the spectrum is that one can distinguish emission from $Hg^{37}Cl$ as well as $Hg^{35}Cl$. Thus in this instance, at least, the ANET approach can be used to quantitate isotopic ratios. Preliminary estimates of our system's sensitivity for $HgCl_2$ detection are in the ppb range.

4.3 Detection of Mercury on Particulates

In our discussion above on the properties of the microdischarges in the D-B discharge, we suggested that the D-B discharge might be able to be used to detect contaminants on particulates such as fly ash or cement. We are currently investigating this possibility. Ultimately two issues need to be addressed. The first is to determine whether or not small concentrations of fine dust particles affect significantly the operation of the dielectric-barrier discharge being used in the ANET process. The second is whether hazardous species adsorbed on the dust particles can be vaporized and subsequently detected in the D-B discharge. Although we have not yet investigated these issues in detail, we were able to demonstrate qualitatively that mercury can indeed be detected on dust particles.

For this test, we used a simulated-cement dust that we spiked by adding a few drops of an aqueous mercury solution to 1-2 g of the dust. The powders used to make the particulate sample were chosen to have the finest possible particle size, generally 10 μm or less. We took spectra of the D-B lamp in the absence of any added dust, and again after we had placed some of the dust sample in one of the gas lines conducting the nitrogen to the D-B lamp. Figure 7 illustrates the results of that test. The spectrum displayed is the difference between two spectra, one taken before the dust was added to the gas feed line subtracted from one taken after dust was added to the feed line. Clearly, the only spectral feature of any significance is the 253.7 nm emission from atomic mercury, thus demonstrating clearly that ANET can be used to detect mercury adhering to particulate samples.

5. CONCLUSIONS

Our results indicate that ANET is a very sensitive technique for monitoring mercury, both free mercury and that tied up with chlorine. Our approach requires no special sample preparation and can operate continuously. In spite of the fluorescence quenching we have observed, the overall sensitivity is well below ppb levels. Thus ANET should prove quite suitable for use as an on-line monitor of mercury levels in flue gases.

ACKNOWLEDGEMENTS

We appreciate financial support for this project from the Department of Energy under an SBIR phase I grant, contract no. DE-FG02-93-ER81528.

REFERENCES

1. Wright, A.N., and Winkler, C.A., Active Nitrogen, New York: Academic Press (1968).
2. Capelle, G.A. and Sutton, D.G., "Metastable Transfer Emission Spectroscopy--Method and Instrument for Detection and Measurement of Trace Materials in Gas Flows," Rev. Sci. Instrum. 49, 1124 (1978).
3. Jurgensen, H. and Winefordner, J.D., "Use of Active Nitrogen in Analytical Chemiluminescence Spectrometry," Talanta 31, 777 (1984).
4. Piper, L.G., Kessler, W.J., Fraser, M.E., and Davis, S.J., "Quantitative Lubricating Oil Debris Monitoring and Analysis," Final Report prepared for Naval Sea Systems Command, PSI-1101/TR-1095, January, 1991.
5. Golde, M.G., "Reactions of $N_2(A\ ^3\Sigma_u^+)$", Int. J. Chem. Kinet. 20, 75-92 (1988).
6. Eliasson, B. and Kogelschatz, U., "The Silent Discharge and its Application to Ozone and Excimer Formation", in Nonequilibrium Processes in Partially Ionized Gases, M.Capitelli and J. N. Bardsley eds., New York: Plenum Press, pp. 401-410 (1990).
7. Braun, E., Küchler, U., and Pietsch, G., "Microdischarges in Air-fed Ozonizers", J. Phys. D.: Appl. Phys. 24, 564 (1991).
8. D'Silva, A.P., Rice, G.W., and Fassel, V.A., "Atmospheric Pressure Active Nitrogen (APAN)-A New Source for Analytical Spectroscopy", Appl. Spectrosc. 34, 578 (1980).
9. Wulf, O.R. and Melvin, E.H., "Band Spectra in Nitrogen at Atmospheric Pressure. A Source of Band Spectra Excitation", Phys. Rev. 55, 687 (1939).
10. Cummings, W.P. and Piper, L.G., "Production of $N_2(A\ ^3\Sigma_u^+)$ in the Low pressure Dielectric-Barrier (Ozonizer) Discharge", Appl. Spectrosc. 44, 656 (1990).
11. Piper, L.G., "Reevaluation of the Transition-Moment function and Einstein Coefficients for the $N_2(A\ ^3\Sigma_u^+ -- X\ ^1\Sigma_g^+)$ Transition," J. Chem. Phys. 99, 3174 (1993).
12. Deech, J.S., Pitre, J., and Krause, L., "Quenching and Depolarization of Mercury Resonance Radiation," Can. J. Phys. 49, 1976 (1971).
13. Dreyer, J.W., and Perner, D., "Deactivation of $N_2(A\ ^3\Sigma_u^+, v=0\text{-}7)$ by Ground State Nitrogen, Ethane, and Ethylene measured by Kinetic Absorption Spectroscopy," J. Chem. Phys. 58, 1195 (1973).
14. Piper, L.G., Caledonia, G.E., and Kennealy, J.P., "Rate Constants for Deactivation of $N_2(A)$ $v'=0,1$ by O_2," J. Chem. Phys. 74, 2888 (1981).
15. Piper, L.G., "Quenching of Metastable Nitrogen Molecules in a Dielectric-Barrier Discharge," manuscript in preparation.
16. Piper, L.G., Shwimer, J.S., Davis, S.J., and Rosen, D.I., "A Compact Vacuum Ultraviolet Light Source Based Upon Dielectric-Barrier Discharge Technology," PSI-2229/TR-1261, final report to NASA/Goddard Space Flight Center under contract no. NASA CR-NASS-32437 (1993).
17. Piper, L.G., Cowles, L.M., Rawlins, W.T., "State-to-State Excitation of $NO(A^2\Sigma^+, v'=0,1,2)$ by $N_2(A\ ^3\Sigma_u^+, v'=0,1,2)$," J. Chem. Phys. 85, 3369 (1986).

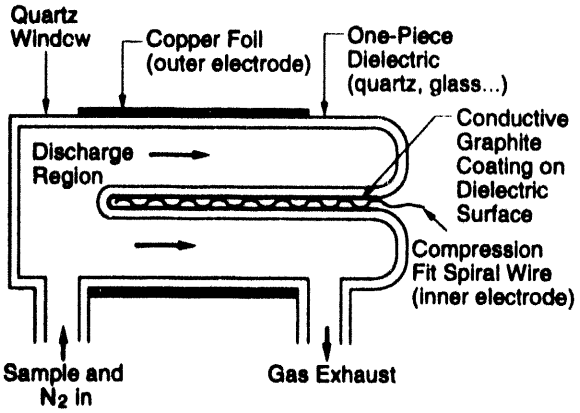

Figure 1. Schematic Diagram of Dielectric-Barrier Discharge Lamp

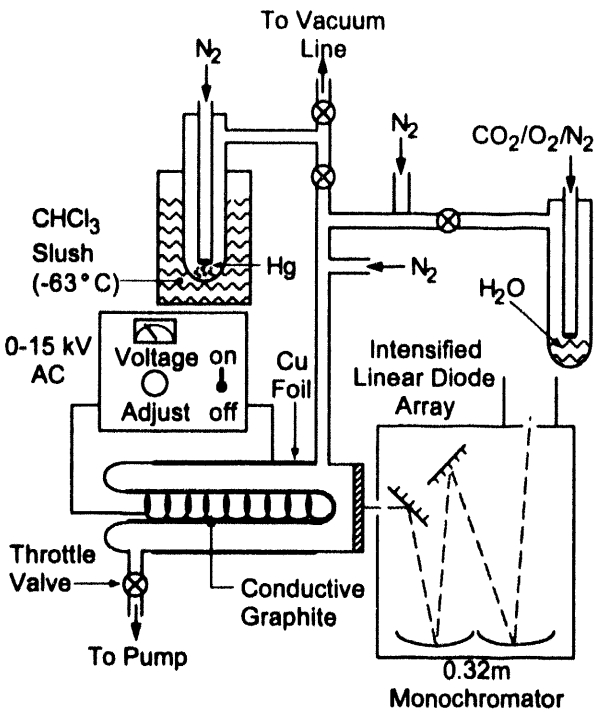

Figure 2. Schematic of Laboratory Apparatus

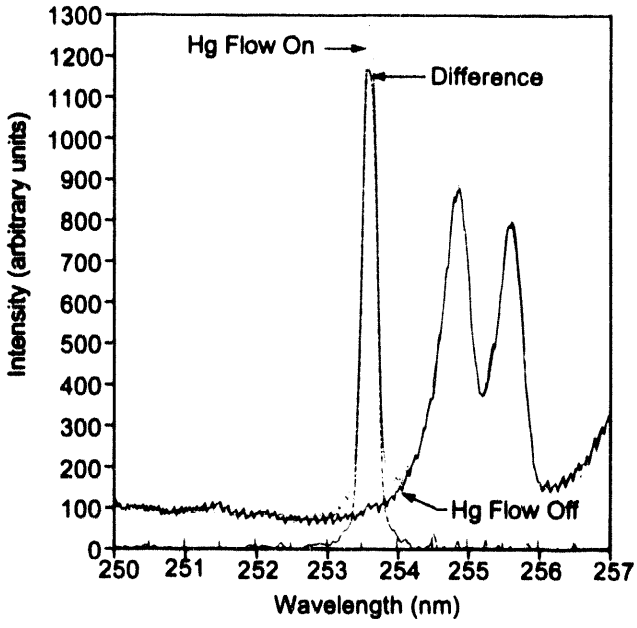

Figure 3a. Spectrum of Dielectric-Barrier Discharge in the Absence and Presence of Added Hg

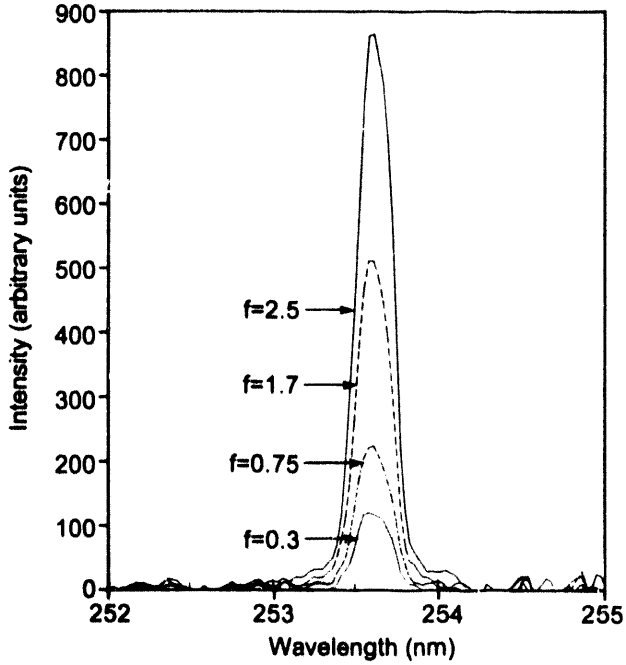

Figure 3b. Background Subtracted D-B Discharge Spectrum in Presence of Hg at Four Different Concentrations

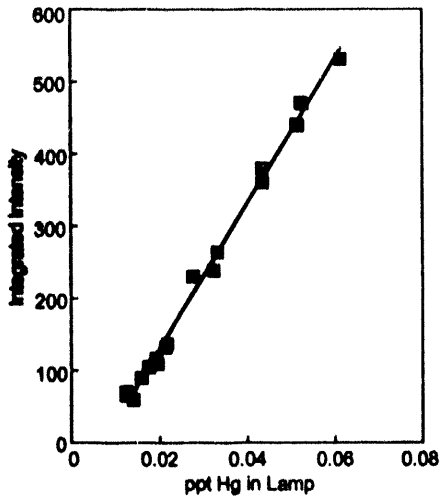

Figure 4. Intensity of Hg 253.7 nm Emission Excited by ANET as a Function of the Mole Fraction of Hg in a D-B Discharge

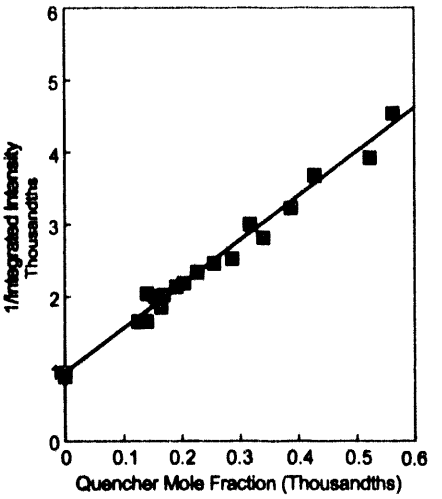

Figure 5. Reciprocal of the Intensity of Hg 253.7 nm Emission in a D-B Discharge as a Function of Mole Fraction of Added Simulated Flue Gas

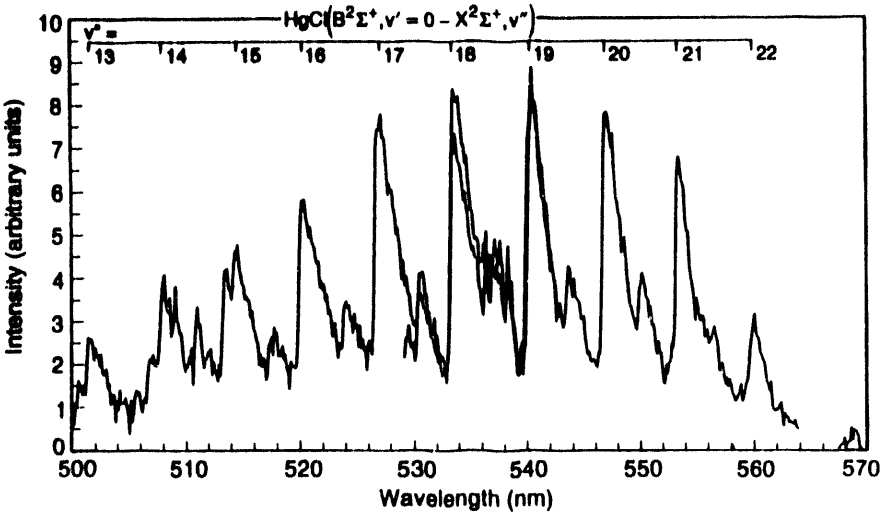

Figure 6. Difference Between D-B Discharge Spectra Taken in the Absence and Presence of $HgCl_2$

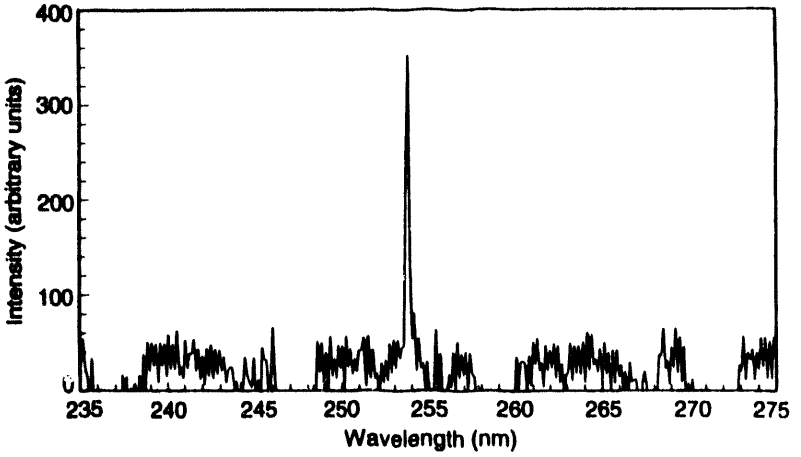

Figure 7. Difference Between D-B Discharge Spectra Taken in the Absence and Presence of Hg-Spiked Dust in the Gas Feed Lines

REAL-TIME ANALYSIS OF TOTAL, ELEMENTAL AND TOTAL SPECIATED MERCURY

RICHARD J. SCHLAGER
SENIOR RESEARCH ENGINEER

MICHAEL D. DURHAM, PH.D.
VICE PRESIDENT, RESEARCH AND TECHNOLOGY

ROGER W. MARMARO
RESEARCH ENGINEER

ADA TECHNOLOGIES, INC.
304 INVERNESS WAY SOUTH, SUITE 110
ENGLEWOOD, CO 80112

Background

Stationary sources in the U.S. emit about 1 million kg of mercury into the atmosphere annually. Major sources of these emissions are fossil fuel combustion facilities and municipal solid waste incinerators. Much work is being done by DOE and industry to characterize these emissions and to develop effective control measures. Continuous emissions monitors (CEMs) for mercury will play a significant role in quickly advancing the level of understanding and control of mercury emissions. Unfortunately, existing CEMs are capable of measuring only the elemental form of mercury, and do not account for speciated mercury compounds.

It is important to understand the nature of mercury emissions for several reasons: 1) different species will require control by different means, and 2) continuous measurement techniques need to account for all mercury species. Determining mercury species emitted from stationary sources has been the subject of much recent work. For example, some researchers believe that the following mercury-containing compounds are found in flue gas generated from the combustion of coal: elemental mercury (Hg^0); mercuric chloride ($HgCl_2$); methyl mercuric chloride (CH_3HgCl); and mercuric oxide (HgO). However, since there is currently no reliable test methods for determining the chemical speciation of mercury as these emissions exit a stationary source stack, the specific quantities and forms of mercury from a given source are not well known (McIlvaine, 1992; Huang, et al., 1991).

Current standard testing techniques rely on manual "grab samples" where flue gas is drawn through filters and traps to collect mercury. The collected samples need to be analyzed in a chemistry laboratory using complex techniques and instrumentation. These field sampling

and analytical techniques are cumbersome, labor intensive, and expensive. A 1-week comprehensive sampling program can cost in the range of $25,000-$50,000.

In response to the need for performing these measurements in real-time, ADA Technologies is developing an analyzer that will be capable of measuring total mercury, elemental mercury, and (by difference) total speciated mercury. Several key analyzer components were evaluated during a Phase I SBIR program. Results show that speciated mercury can be converted to elemental mercury using a proprietary conversion technique, and elemental mercury can be measured at concentrations below 1 $\mu g/m^3$ (less than 0.1 ppb v/v). Figure 1 shows how the analyzer will be used to measure mercury levels upstream and downstream of control devices.

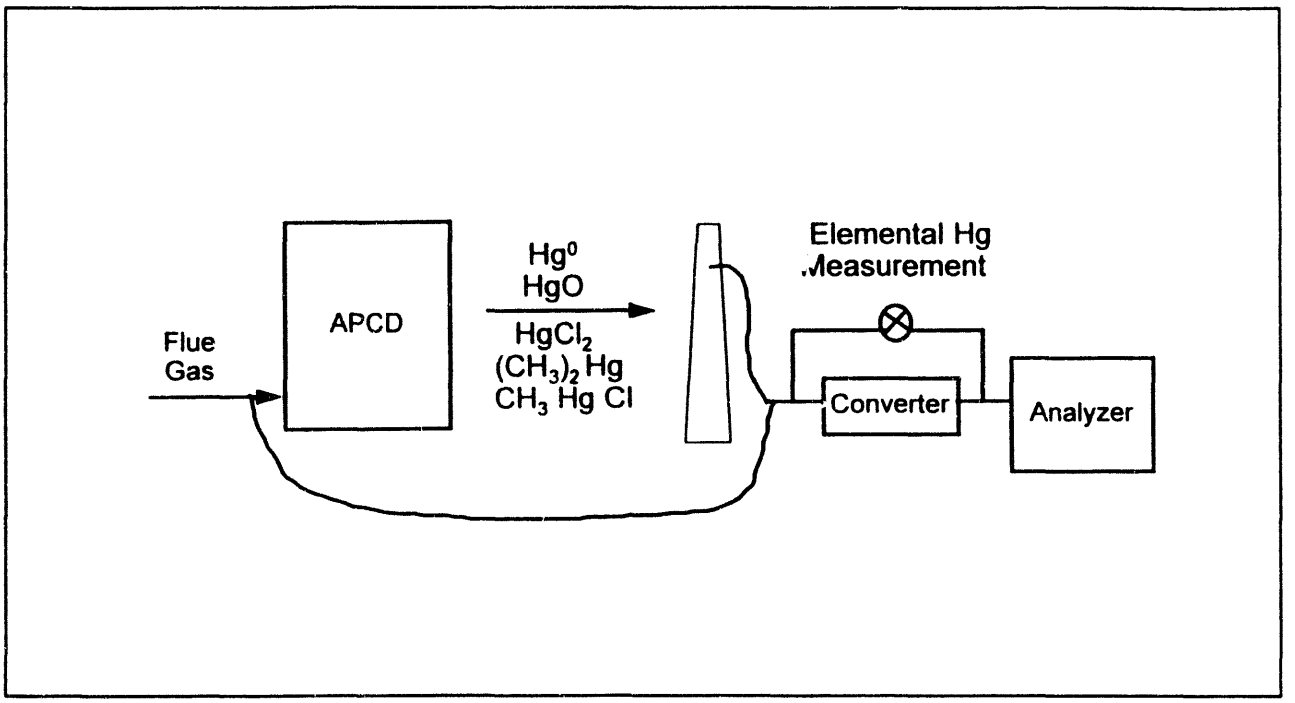

Figure 1. Monitoring mercury concentrations in flue gas.

Approach

The primary objective of the program is to develop a commercial analyzer capable of continuously monitoring concentrations of total, elemental, and speciated mercury in flue gas. The approach used during Phase I was to evaluate a technique for converting speciated forms of mercury to elemental mercury, and to provide specifications for integrating the converter with a mercury CEM. Total mercury is measured by passing the flue gas sample through the converter. Elemental mercury concentrations are measured by the CEM when the flue gas sample bypasses the pre-conditioning converter. Total speciated mercury is then determined as the difference between the measured total mercury concentration and the elemental mercury concentration.

Phase I testing was performed in a laboratory experimental program, involving the generation of quantitative amounts of elemental and several speciated mercury compounds. A technique was investigated for converting the speciated forms of mercury to the elemental form. The effectiveness of the conversion process was determined using a real-time elemental mercury analyzer.

Experimental

Figure 2 shows the laboratory apparatus used during the program. A gas matrix was generated from certified compressed gases. For a majority of the early screening tests, compressed air was used. Later tests were performed using typical flue gas constituents.

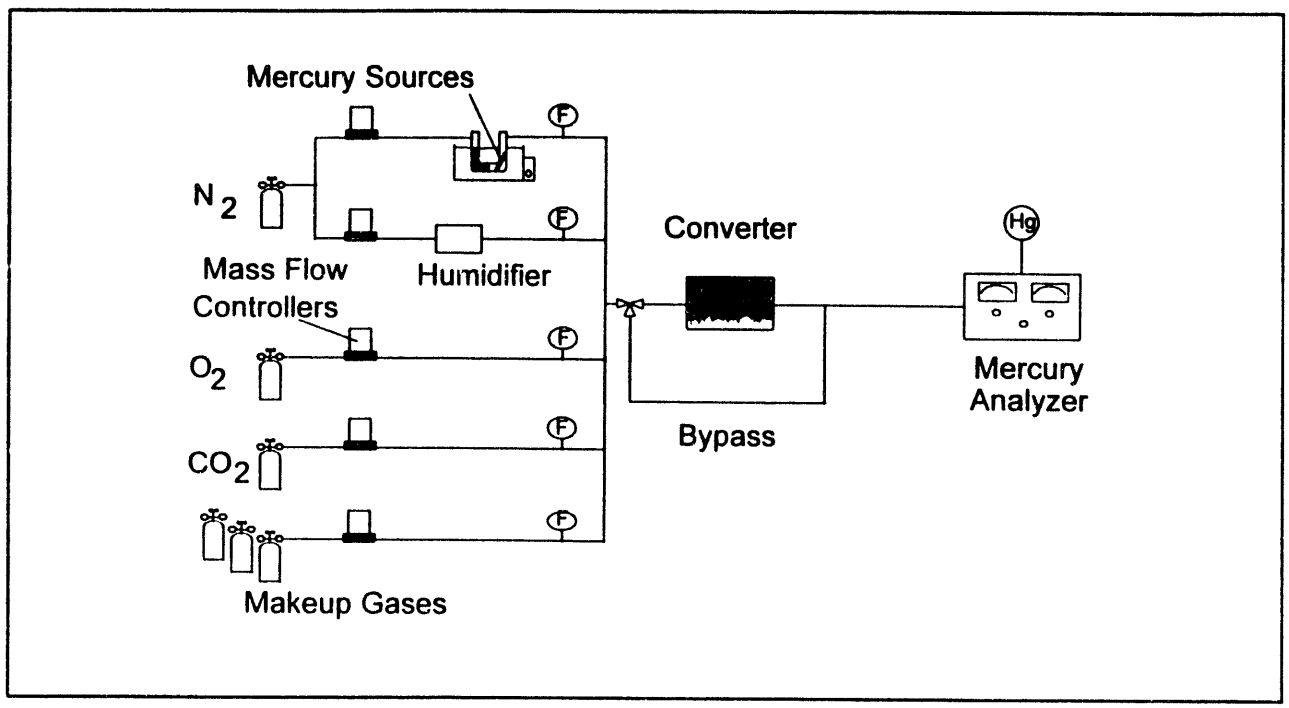

Figure 2. Schematic diagram of laboratory test fixture.

Three mercury sources were used during the testing: 1) elemental mercury, 2) dimethyl mercury, and 3) mercuric chloride. Permeation tubes were used to generate elemental mercury and dimethyl mercury vapor. A diffusion vial was fabricated to generate mercuric chloride vapor. These sources were calibrated by periodically weighing them using an analytical balance. Constant permeation rates were obtained after a suitable stabilization period. Dimethyl mercury was selected as a surrogate for organo-mercury species, and mercuric chloride was used as a surrogate for ionic mercury species. It is widely believed that elemental mercury and mercuric chloride are the two most predominant species in flue gases generated from coal combustion.

The flow rate of the test gas was approximately 1 lpm. The concentration of the mercury sources ranged from 4.5 $\mu g/m^3$ to 50 $\mu g/m^3$ (0.7 ppb to 9 ppb v/v). Different

converter parameters were evaluated to determine optimum operating conditions (as gauged by quantitative mercury species conversion rates). In addition, several mercury detection systems were tested to determine capabilities.

Three elemental mercury detection methods were evaluated during the program. All operate on the principle of ultraviolet (UV) radiation absorption. Elemental mercury absorbs UV at a wavelength of 253.7 nm, and the amount of radiation absorbed is proportional to the concentration of elemental mercury. The goal of evaluating different mercury detectors was to define a design that is capable of providing the desired level of sensitivity for the measurements. The target for the detector was to be capable of measuring mercury concentrations down to 1 $\mu g/m^3$ (approximately 0.1 ppb v/v).

Results

Converter. An optimum converter design was established based on the testing. An elemental mercury analyzer was used to determine whether mercuric chloride and dimethyl mercury were being converted to elemental mercury. Tests showed that these two species would not produce a signal in the analyzer if they were input without first passing through the converter. Figures 3 and 4 show analyzer response when these compounds were passed through the converter. The test sequence followed the pattern of placing the mercury species through the converter, then the bypass valve was actuated to circumvent the converter. This sequence was followed for a number of cycles to establish the fact that the mercury compounds were being converted to elemental mercury.

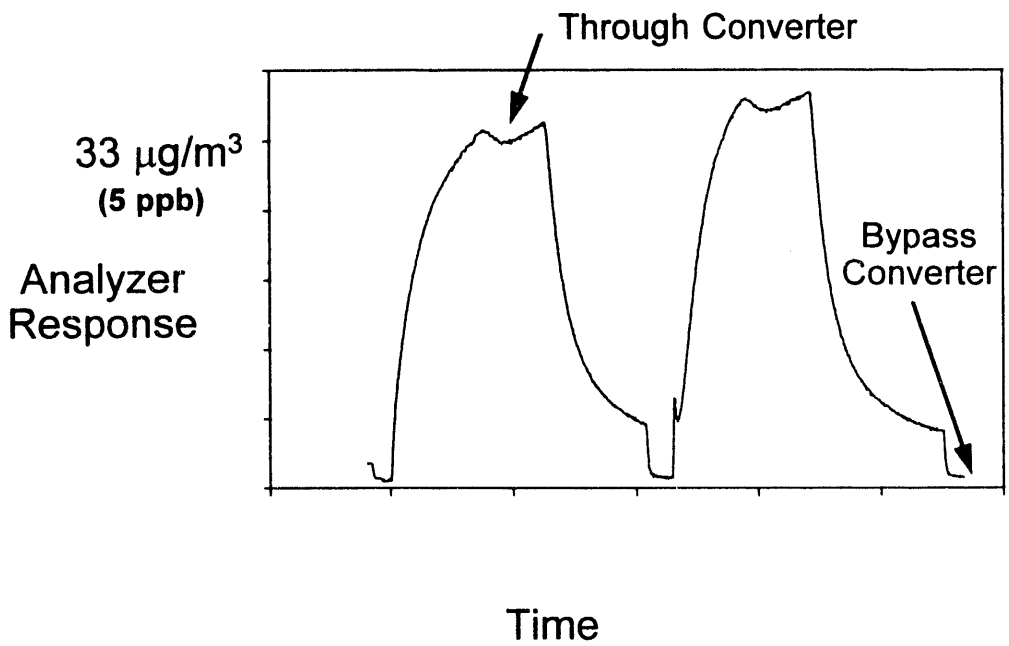

Figure 3. Results of mercuric chloride being converted to elemental mercury.

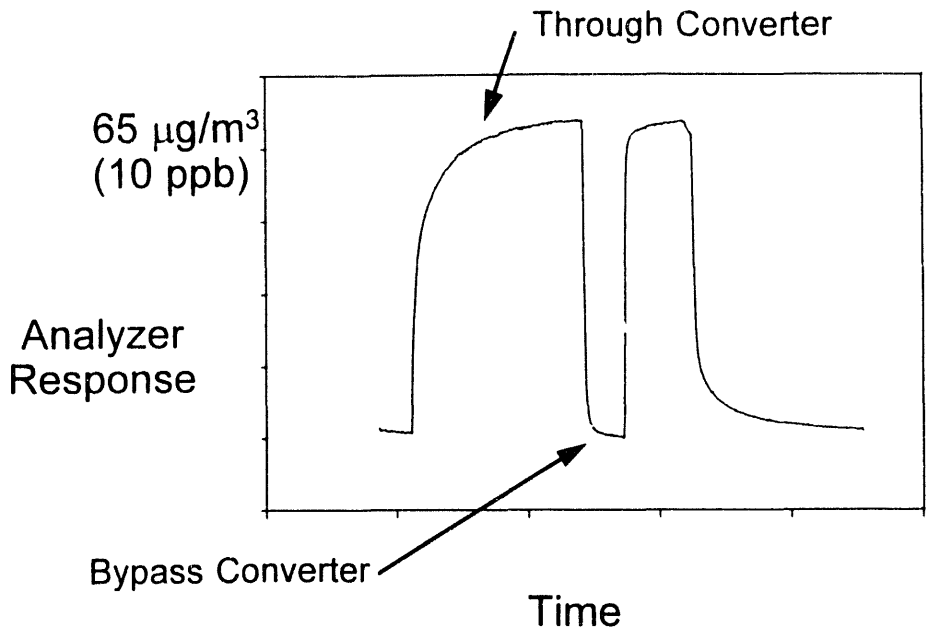

Figure 4. Results of dimethyl mercury being converted to elemental mercury.

Mercury Detector. An early goal of the program was to establish the capability of measuring mercury at a level of 1 $\mu g/m^3$ (approx. 0.1 ppb v/v). Three different UV absorption spectrometer configurations were evaluated to determine which was most suitable for providing this capability. One spectrometer, based on a unique source modulation technique, showed excellent rejection of interferences and an extremely low limit of detection. Figure 5 shows the analyzer response when elemental mercury was introduced at a concentration of 4.2 $\mu g/m^3$ (0.7 ppb v/v). Also shown is the signal when zero gas was introduced into the analyzer. Based on the peak-to-peak noise level observed, a minimum level of detection (defined as 2x noise level) of 0.2 $\mu g/m^3$ (27 ppt v/v).

The response of the analyzer was also determined over a range of elemental mercury concentrations as shown in Figure 6. The response of the analyzer is linear between the concentration range tested (0 to 6 ppb v/v). This range is expected to cover most concentrations expected in coal-fired flue gases.

Future Plans

Based on the successful results of the Phase I effort, ADA has recommended the continuation of the work in a Phase II program. During Phase II, a prototype CEM system will be fabricated and field demonstrated at a number of sites. A commercialization partner will participate throughout the program in key tasks relative to introducing a reliable commercial product at the end of the two-year project.

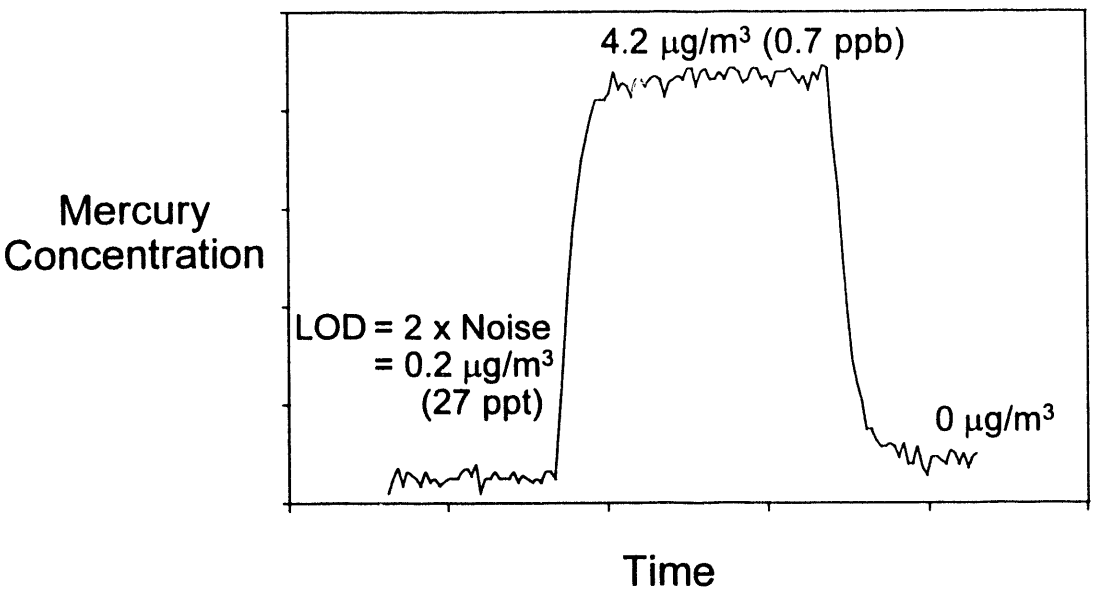

Figure 5. Test to determine minimum level of detection of the mercury detector.

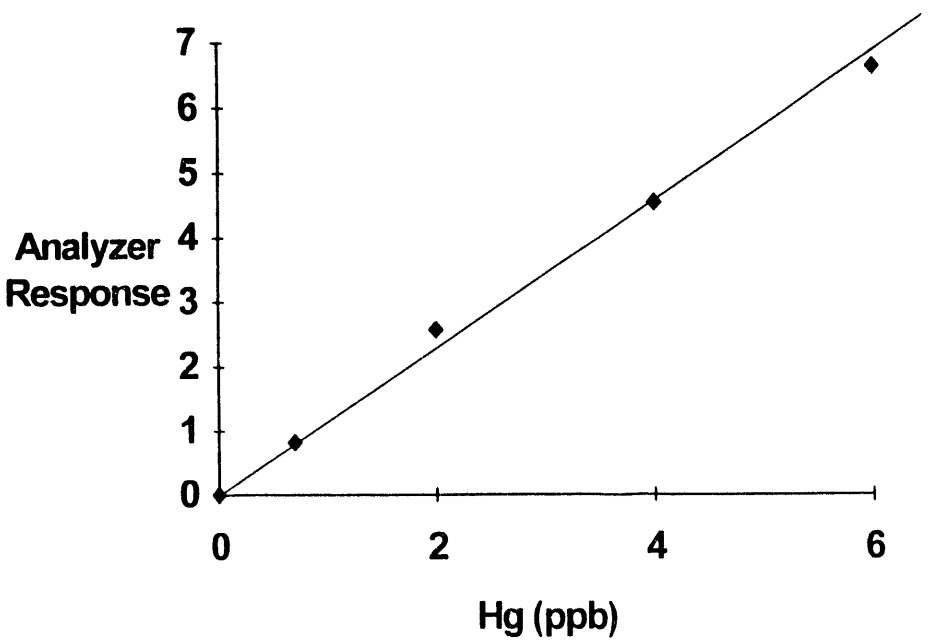

Figure 6. Linearity of the mercury detector.

Conclusions

Following are conclusions based on the results of the program to date:

- Mercuric chloride and dimethyl mercury are quantitatively converted to elemental mercury using a conversion technique.
- Once converted, these compounds can be measured using a UV absorption spectrometer.
- The minimum level of detection of the mercury detector is 0.2 $\mu g/m^3$ (27 ppt v/v).

References

Huang, H.S., C.D. Livengood and S. Zaromb (1991). "Emissions of Airborne Toxics From Coal-Fired Boilers: Mercury", Report No. ANL/ESD/TM-35, U.S. Department of Energy, September.

McIlvaine Company (1992). "Mercury Speciation is Important and Doable", *Air Pollution Monitoring and Sampling Newsletter*, No. 147, January.

The following manuscript was unavailable at the time of publication.

CONTROL OF MERCURY AND OTHER VOLATILE TRACE METALS IN FOSSIL-FUEL-FIRED POWER GENERATION

J. R. Morency
PSI Technology
20 New England Business Center
Andover, MA 01810

Please contact author(s) for a copy of this paper.

AUTHORS INDEX

AUTHORS INDEX

A

B

C

D

E

F

G

H

J

K

L

M

N

O

P

R

S

T

V

W

X

Y

Z